



Sharif University of Technology
Scientia Iranica
Transactions A: Civil Engineering
<http://scientiairanica.sharif.edu>



Control of natural frequency of beams using different pre-tensioning cable patterns

N. Fanaie* and F. Partovi

Department of Civil Engineering, K.N. Toosi University of Technology, Tehran, Iran.

Received 24 May 2018; received in revised form 29 September 2018; accepted 9 March 2019

KEYWORDS

Natural frequency;
 Steel beam;
 Cable;
 Pre-tensioning;
 Least work;
 Rayleigh's method.

Abstract. Sometimes, natural frequency of beams is not within the allowable range despite the appropriate shear and bending design. Every so often, structural designers face cases in which it is not possible to increase the beam height. Steel cable is utilized in this research to control the natural frequency of beam due to its important advantages such as low weight, small cross-sectional area, and high tensile strength. For the first time, theoretical relations were developed to calculate the rate of increase in pre-tensioning force of steel cables under external loading based on the method of least work. Moreover, the natural frequency of steel beams with different support conditions without cable and with different patterns of cable was calculated based on Rayleigh's method. To verify the theoretical relations involved, the steel beam was modeled using ABAQUS software. The obtained results showed that the theoretical relations could appropriately predict the natural frequency of beams with different support conditions and cable patterns. In addition, simply supported and fixed supported beams were prestressed with V-shaped and modified V-shaped patterns of the cable. According to the obtained results, the modified V-shaped pattern of the cable was more efficient than the V-shaped pattern.

© 2020 Sharif University of Technology. All rights reserved.

1. Introduction

Reckoned as important components of a structure, cables are materials that can tolerate tensile force and generally increase the stiffness and bearing capacity of a structure [1]. Nowadays, cables are increasingly used in structures. Hou and Tagawa applied cable-cylinder bracing to the seismic retrofitting of steel flexural frames. From their viewpoint, through this retrofitting method, the lateral strength of the storey increases without decreasing the ductility of flexural

frame [2]. Fanaie et al. presented theoretical relations for the cable-cylinder bracing system using a rigid steel cylinder. They verified the results using finite element ABAQUS software [3]. They also studied seismic behavior of steel flexural frames strengthened with cable-cylinder bracing and obtained reasonable results [4]. Giaccu investigated the non-linear dynamic behavior of pre-tensioned-cable cross-braced structures in the presence of slackening in the braces. They concluded that there was a direct correlation between equivalent frequency and slackening in the braces [5].

Pre-tensioning of steel beams through high-strength cables is one of the most efficient methods for reducing the required steel and increasing their bearing capacity. The pre-tensioning technique was primarily used for reinforced concrete structures; however, for the first time, it was utilized by Dischinger and Magnel

*. Corresponding author. Tel.: +98 21 88779473
 E-mail addresses: fanaie@kntu.ac.ir (N. Fanaie),
he.partovi@gmail.com (F. Partovi)

for steel beams. Pre-tensioned steel structures are constructed all over the world, especially in America, Russia, and Germany. This fact shows the greater structural and economic merits of prestressed steel beams than non-prestressed ones. The pre-tensioning technique is appropriate for constructing new structures and strengthening the existing ones [6].

Some researchers have studied prestressed beams using tendons. Le et al. experimentally evaluated the application of either unbonded Carbon Fibre Reinforced Polymer (CFRP) tendons or steel tendons to precast T-section segmental concrete beams and tested them under cyclic loads. They concluded that CFRP tendons could easily replace steel tendons so that beams could achieve both high strength and ductility capacity [7]. Pisani analyzed simply supported concrete beams externally prestressed under sustained loads and introduced two numerical methods to describe the time evolution of both stress distribution and displacement of a simply supported concrete beam externally prestressed. Besides, they presented an example to verify the precision of the methods [8]. Lou et al. numerically studied the flexural response of continuous externally fiber reinforced polymer prestressed concrete beams with various linearly transformed cable profiles. They observed that the cable shift by linear transformation did not affect the basic performance at all stages of loading up to failure and the secondary moments varied linearly with the cable shift [9]. Nie et al. presented theoretical relations to calculate the deflection as well as yield and ultimate moments of simply supported prestressed steel-concrete composite beam, considering the slip effect. They verified the suggested formulas with experimental results [10]. Zhou et al. conducted an experimental study and applied the numerical model of prestressed composite beams subjected to fire and positive moment. They observed that the fire resistance of composite beams prestressed with external tendons was highly influenced by the stress in the cable strands [11]. Troitsky evaluated the behavior of prestressed steel beam using cables and observed an increase in the stiffness and a decrease in the deformation of the beam [6]. Belletti and Gasperi studied the behavior of prestressed simply supported steel I-shaped beams by tendons with focus on two parameters: the number of deviators and the value of prestressing force [12]. Park et al. analytically and experimentally evaluated the flexural behavior of steel I-beam prestressed with externally unbonded tendons. They observed a considerable increase in the yielding and ultimate bearing capacity of steel I-beam [13]. Kambal and Jia derived a finite-element formulation to investigate the effectiveness of applying the prestressing technique with respect to the flexural behavior of a simply supported steel box girder and they verified it based on experimental

results [14]. Zhang examined the analytical solutions of the symmetric and antisymmetric elastic lateral-torsional buckling of prestressed steel I-beams with rectilinear tendons under equal end moments and verified the correctness of the analytical solutions based on the solutions simulated using ANSYS [15].

A number of researchers have investigated the dynamic behavior of pre-tensioned beams. Noble et al. studied the results of dynamic impact testing on externally axially loaded steel Rectangular Hollow Sections (RHSs) and compared the response to those of externally post-tensioned steel RHSs. Moreover, they tested the validity of the “compression-softening” effect for post-tensioned sections. They concluded that the “compression-softening” theory was not valid for pre- or post-tensioned sections [16]. Cao et al. investigated the vibration performance of the arch prestressed concrete truss girder subjected to the on-site heel-drop and jumping impact tests and carried out theoretical analyses. They concluded that the theoretical fundamental natural frequency was in general agreement with the experimental result [17]. Miyamoto et al. studied the dynamic behavior of the pre-tensioned simply supported composite beam with external tendon. They derived the natural frequency equation of the pre-tensioned beam based on the flexural vibration equation and verified the predicted equation by comparing it with the results of the dynamic experiment [18]. Park et al. analytically and experimentally studied the strengthening effect of bridges using external pre-tensioned tendons and concluded that strengthening would reduce the mid-span deflection by 10–24% [19].

To control the natural frequency of the beam, structural designers have faced cases in which it is not possible to increase the beam height due to architectural limitations, or cases in which beam frequency limitation was not considered during design and the problem of vibration was observed after implementation. In this study, the natural frequency of steel beams was evaluated without cable and with various support conditions and different cable patterns.

The increase in pre-tensioning force of steel cable subjected to external loading is determined using method of least work. Then, Rayleigh’s method is applied to developing the natural frequency relations of steel beam equipped with the cable. In order to validate the obtained natural frequency relations, the results of theoretical relations are compared with those of finite element model of the beams.

2. Pre-tensioning symmetric I-shaped steel beam with steel cable

Symmetric I-shaped steel beam was considered in different support conditions, namely simply supported

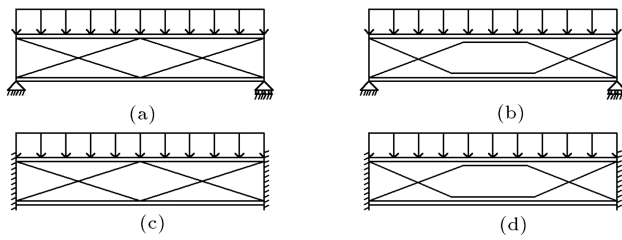


Figure 1. Prestressed symmetric I-shaped steel beams with steel cable under external loading: (a) Simply supported beam along with V-shaped cable pattern, (b) simply supported beam along with modified V-shaped cable pattern, (c) fixed supported beam along with V-shaped cable pattern, and (d) fixed supported beam along with modified V-shaped cable pattern.

and fixed supported beams. As shown in Figure 1, prestressed cables with different patterns were used on both sides of beam web subjected to external loading. In the frequency analysis, beam movement is of back and forth types; therefore, as observed in the figure, regarding the V-shaped pattern, the cable was fixed at both ends to one of the flange (top or bottom) of the beam on both sides of the web. Then, in the middle of the beam, it passes through the reel on the another flange causing the pattern with two inclined cables. Moreover, in the modified V-shaped pattern, the cable remains fixed at both ends to the one of flange (top or bottom) of the beam on both sides of the web and then, it passes through two reels on another flange producing a pattern with one horizontal cable in the middle and two inclined ones on each side.

The following assumptions are taken into account to analyze the prestressed symmetric I-shaped steel beams with steel cable:

1. The materials of steel beam and cable are linearly elastic;
2. The deformations are small;
3. Shear deformation is neglected;
4. The friction loss in the region of the cable deformation and the relaxation of steel cable are ignored;
5. Steel beam section is rolled; therefore, it is compact.

3. Natural frequency

The natural frequency of systems with distributed mass and rigidity, which are usually considered as single-degree-of-freedom systems and also known as generalized single degree of freedom systems, can be calculated using Rayleigh's method. This method is based on the principle of conservation of energy. The principle of conservation of energy states that the total energy in a freely vibrating undamped system is constant (i.e., it does not vary with time).

4. Calculating the natural circular frequency of beam by Rayleigh's method

The simple harmonic motion of a beam under free vibration can be defined as follows:

$$u(x, t) = z_o \psi(x) \sin \omega_n t', \quad (1)$$

where $\psi(x)$ is an assumed shape function defining the form of deflections and satisfying the displacement boundary conditions. The shape function can be determined from deflections using a selected set of static forces. One common selection of these forces is the weight of structure applied in an appropriate direction. Moreover, z_o is the amplitude of generalized coordinate $z(t)$ and ω_n is the natural circular frequency of beam. The velocity of beam is equal to the following:

$$\dot{u}(x, t) = \omega_n z_o \psi(x) \cos \omega_n t'. \quad (2)$$

The maximum potential energy of the system over a vibration cycle is equal to its strain energy associated with the maximum displacement $u_o(x)$:

$$E_{So} = \int_0^L \frac{1}{2} EI(x) [u_o''(x)]^2 dx. \quad (3)$$

The maximum kinematic energy of the system over a vibration cycle is associated with the maximum velocity $\dot{u}_o(x)$:

$$E_{Ko} = \int_0^L \frac{1}{2} m(x) [\dot{u}_o(x)]^2 dx. \quad (4)$$

Through Eqs. (1) and (2), the maximum displacement $u_o(x)$ and maximum velocity $\dot{u}_o(x)$ are defined as follows:

$$u_o(x) = z_o \psi(x), \quad (5)$$

$$\dot{u}_o(x) = \omega_n z_o \psi(x) = \omega_n u_o(x). \quad (6)$$

The natural circular frequency of beams is obtained by replacing Eqs. (5) and (6) in Eqs. (3) and (4); besides, by using the principle of conservation of energy, equating the maximum strain energy, E_{So} , to maximum kinematic energy E_{Ko} gives:

$$\omega_n^2 = \frac{\int_0^L EI(x) [\psi''(x)]^2 dx}{\int_0^L m(x) [\psi(x)]^2 dx}, \quad (7)$$

where $m(x)$ is the mass per unit length of the beam, $EI(x)$ flexural rigidity, and L the beam length.

Eq. (7) is Rayleigh's quotient for a system with distributed mass and rigidity. Rayleigh's method can be used to calculate the natural frequency of beam with different support conditions without cable and different patterns of cable.

4.1. Calculating the natural frequency of the simply supported beam without cable

To determine the shape function of the simply supported beam, as shown in Figure 2(a), the boundary conditions are as follows:

$$u_o(0) = u_o(l_b) = 0, \quad u'_o\left(\frac{l_b}{2}\right) = 0.$$

With this limitation, two different shape functions can be assumed.

4.1.1. Calculating the natural frequency of the simply supported beam based on the assumed shape function

The hypothetical shape function satisfying the displacement boundary conditions is considered as follows:

$$\psi(x) = \sin \frac{\pi x}{l_b}. \quad (8)$$

The natural circular frequency of the simply supported beam is obtained using Rayleigh's quotient formula (Eq. (7)) by replacing the assumed shape function according to Eq. (8) as follows:

$$\begin{aligned} \omega_n^2 &= \frac{\int_0^{l_b} EI(x) [\psi''(x)]^2 dx}{\int_0^{l_b} m(x) [\psi(x)]^2 dx} \\ &= \frac{(EI)_b \int_0^{l_b} \left(-\frac{\pi^2}{l_b^2} \sin \frac{\pi x}{l_b}\right)^2 dx}{\frac{q_D}{g} \int_0^{l_b} \left(\sin \frac{\pi x}{l_b}\right)^2 dx} = \frac{\pi^4 (EI)_b g}{l_b^4 q_D} \\ &\rightarrow \omega_n = \frac{\pi^2}{l_b^2} \sqrt{\frac{(EI)_b g}{q_D}}, \end{aligned} \quad (9)$$

where $m(x)$ is the mass per unit length equal to $\frac{q_D}{g}$ (q_D is the uniform dead load per unit length and g is the gravity acceleration), l_b is the beam length, and $(EI)_b$ is the flexural rigidity of the beam.

The natural frequency of the simply supported beam is obtained using the natural circular frequency formula (Eq. (9)) as follows:

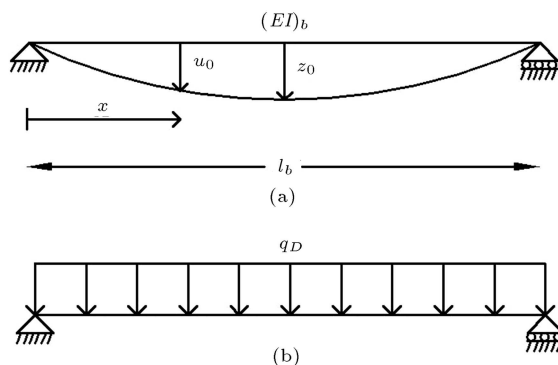


Figure 2. (a) Deflection curve of the simply supported beam. (b) Simply supported beam subjected to vertical structural weight.

$$f = \frac{\omega_n}{2\pi} = \frac{\pi}{2l_b^2} \sqrt{\frac{(EI)_b g}{q_D}}. \quad (10)$$

4.1.2. Calculating the natural frequency of the simply supported beam based on the shape function resulting from the deflection curve

A possible approach is to select the shape function based on the deflection curve due to static force. The bending moment equation of the simply supported beam due to vertical structural weight (as in Figure 2(b)) in order to determine the deflection curve is as follows:

$$M(x) = \frac{q_D l_b x}{2} - \frac{q_D x^2}{2}. \quad (11)$$

The internal bending moment is equal to:

$$M(x) = -(EI)_b u''_o(x). \quad (12)$$

By replacing Eq. (11) in Eq. (12) and imposing boundary conditions, the deflection curve is obtained as follows:

$$u_o(x) = \frac{5q_D l_b^4}{384(EI)_b} \left[\frac{16}{5} \left(\frac{x}{l_b}\right) - \frac{32}{5} \left(\frac{x}{l_b}\right)^3 + \frac{16}{5} \left(\frac{x}{l_b}\right)^4 \right]. \quad (13)$$

If the deflection in the mid-span of the simply supported beam (as Figure 2(a)) is assumed as the amplitude of generalized coordinate $z_o = u_o\left(\frac{l_b}{2}\right) = \frac{5q_D l_b^4}{384(EI)_b}$, the shape function is obtained as follows:

$$\psi(x) = \frac{16}{5} \left(\frac{x}{l_b}\right) - \frac{32}{5} \left(\frac{x}{l_b}\right)^3 + \frac{16}{5} \left(\frac{x}{l_b}\right)^4. \quad (14)$$

The natural circular frequency of the simply supported beam using Rayleigh's quotient formula (Eq. (7)) by replacing the obtained shape function from the deflection curve according to Eq. (14) is obtained as follows:

$$\begin{aligned} \omega_n^2 &= \frac{\int_0^{l_b} EI(x) [\psi''(x)]^2 dx}{\int_0^{l_b} m(x) [\psi(x)]^2 dx} \\ &= \frac{(EI)_b \int_0^{l_b} \left(-\frac{192x}{5l_b^3} + \frac{192x^3}{5l_b^4}\right)^2 dx}{\frac{q_D}{g} \int_0^{l_b} \left(\frac{16}{5} \left(\frac{x}{l_b}\right) - \frac{32}{5} \left(\frac{x}{l_b}\right)^3 + \frac{16}{5} \left(\frac{x}{l_b}\right)^4\right)^2 dx} \\ &= \frac{3024(EI)_b g}{31l_b^4 q_D} \rightarrow \omega_n = \frac{12}{l_b^2} \sqrt{\frac{21(EI)_b g}{31q_D}}. \end{aligned} \quad (15)$$

Then, the natural frequency of the simply supported beam is obtained as follows:

$$f = \frac{\omega_n}{2\pi} = \frac{6}{\pi l_b^2} \sqrt{\frac{21(EI)_b g}{31q_D}}. \quad (16)$$

4.2. Calculating the natural frequency of the fixed supported beam without cable

To determine the shape function of the fixed supported beam, as shown in Figure 3(a), the boundary conditions are given below:

$$u_o(0) = u_o(l_b) = 0, \quad u'_o(0) = u'_o\left(\frac{l_b}{2}\right) = u'_o(l_b) = 0.$$

Considering this limitation, two different shape functions can be assumed.

4.2.1. Determining the natural frequency of the fixed supported beam based on assumed shape function

The assumed shape function satisfying the displacement boundary conditions is considered as follows:

$$\psi(x) = 1 - \cos \frac{2\pi x}{l_b}. \quad (17)$$

The natural circular frequency of the fixed supported beam using Rayleigh's quotient formula (Eq. (7)) by replacing the assumed shape function according to Eq. (17) is obtained as follows:

$$\begin{aligned} \omega_n^2 &= \frac{\int_0^{l_b} EI(x) [\psi''(x)]^2 dx}{\int_0^{l_b} m(x) [\psi(x)]^2 dx} \\ &= \frac{(EI)_b \int_0^{l_b} \left(\frac{4\pi^2}{l_b^2} \cos \frac{2\pi x}{l_b} \right)^2 dx}{\frac{q_D}{g} \int_0^{l_b} \left(1 - \cos \frac{2\pi x}{l_b} \right)^2 dx} = \frac{16\pi^4 (EI)_b g}{3l_b^4 q_D} \\ &\rightarrow \omega_n = \frac{4\pi^2}{l_b^2} \sqrt{\frac{(EI)_b g}{3q_D}}. \end{aligned} \quad (18)$$

Then, the natural frequency of the fixed supported beam is obtained as follows:

$$f = \frac{\omega_n}{2\pi} = \frac{2\pi}{l_b^2} \sqrt{\frac{(EI)_b g}{3q_D}}. \quad (19)$$

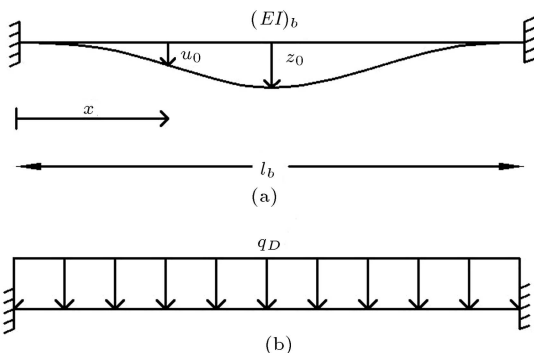


Figure 3. (a) Deflection curve of fixed supported beam. (b) Fixed supported beam subjected to vertical structural weight.

4.2.2. Calculating the natural frequency of the fixed supported beam based on the shape function obtained from the elastic curve

The bending moment equation of the fixed supported beam due to vertical structural weight (as in Figure 3(b)) in order to determine the deflection curve is given below:

$$M(x) = -\frac{q_D l_b^2}{12} + \frac{q_D l_b x}{2} - \frac{q_D x^2}{2}. \quad (20)$$

The internal bending moment is equal to:

$$M(x) = -(EI)_b u''_o(x). \quad (21)$$

By replacing Eq. (20) in Eq. (21) and imposing boundary conditions, the deflection curve is obtained as follows:

$$u_o(x) = \frac{q_D l_b^4}{384(EI)_b} \left[16 \left(\frac{x}{l_b} \right)^2 - 32 \left(\frac{x}{l_b} \right)^3 + 16 \left(\frac{x}{l_b} \right)^4 \right]. \quad (22)$$

If the deflection at the mid-span of the fixed supported beam (as in Figure 3(a)) is assumed as a amplitude of generalized coordinate $z_o = u_o\left(\frac{l_b}{2}\right) = \frac{q_D l_b^4}{384(EI)_b}$, the shape function is obtained as follows:

$$\psi(x) = 16 \left(\frac{x}{l_b} \right)^2 - 32 \left(\frac{x}{l_b} \right)^3 + 16 \left(\frac{x}{l_b} \right)^4. \quad (23)$$

The natural circular frequency of the fixed supported beam using Rayleigh's quotient formula (Eq. (7)) by replacing the shape function obtained from the deflection curve according to Eq. (23) is obtained as follows:

$$\begin{aligned} \omega_n^2 &= \frac{\int_0^{l_b} EI(x) [\psi''(x)]^2 dx}{\int_0^{l_b} m(x) [\psi(x)]^2 dx} \\ &= \frac{(EI)_b \int_0^{l_b} \left(\frac{32}{l_b^2} - \frac{192x}{l_b^3} + \frac{192x^2}{l_b^4} \right)^2 dx}{\frac{q_D}{g} \int_0^{l_b} \left(16 \left(\frac{x}{l_b} \right)^2 - 32 \left(\frac{x}{l_b} \right)^3 + 16 \left(\frac{x}{l_b} \right)^4 \right)^2 dx} \\ &= \frac{504(EI)_b g}{l_b^4 q_D} \rightarrow \omega_n = \frac{6}{l_b^2} \sqrt{\frac{14(EI)_b g}{q_D}}. \end{aligned} \quad (24)$$

Then, the natural frequency of the fixed supported beam is obtained as follows:

$$f = \frac{\omega_n}{2\pi} = \frac{3}{\pi l_b^2} \sqrt{\frac{14(EI)_b g}{q_D}}. \quad (25)$$

4.3. Calculating the natural frequency of the simply supported beam with V-shaped cable pattern

One possible approach to selecting the shape function

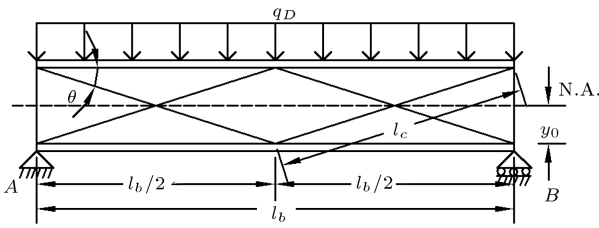


Figure 4. Simply supported beam with the V-shaped cable pattern.

in order to calculate natural frequency of the beam with cable using Rayleigh's method is based on the deflection curve due to static force. One common selection of these forces is the weight of structure applied in the vertical direction.

The cable length increased by Δl and its pre-tensioning force, F_{pt} , increased by ΔF in beams with cable under uniform dead load. Given that the structure is statically indeterminate, the static equilibrium equations are not enough to calculate ΔF . The rate of increase in the force in the cable can be calculated using the method of least work.

Regarding the simply supported beam with V-shaped pattern cable, as shown in Figure 4, the increase in pre-tensioning force of the steel cable is equal to ΔF . Therefore, the axial force of the beam is equal to $\Delta F \cos \theta$. Moreover, with regard to the symmetry of the structure and loading (as in Figure 4), the maximum strain energy of the simply supported beam with V-shaped pattern of cable including strain energy resulting from bending and axial force of the beam and strain energy from axial force of the cable can be obtained for half of the beam. By duplicating it, the maximum strain energy for the whole beam is obtained as follows:

$$E_{So} = 2 \times \frac{1}{2(EI)_b} \int_0^{\frac{l_b}{2}} M(x)^2 dx + 2 \times \frac{\Delta F^2 l_c}{2(AE)_c} + \frac{(\Delta F \cos \theta)^2 l_b}{2(AE)_b}, \quad (26)$$

where l_b and l_c are the lengths of beam and inclined cable, A_b and A_c are cross-section areas of beam and cable on both sides of the web, E_b and E_c are the elasticity moduli of beam and cable, respectively, and I_b is the moment of inertia of beam, θ is the angle of inclined cable with the horizontal axis, and $M(x)$ is the bending moment of the simply supported beam with the V-shaped pattern of cable in the range of $0 \leq x \leq \frac{l_b}{2}$.

Due to the symmetry of structure and loading, the bending moment diagram for the right half of the beam is exactly similar to the left half of the beam; therefore, the bending moment of the simply supported beam with the V-shaped pattern of the cable under uniform distributed dead load for the half of the beam is determined as follows:

For the $0 \leq x \leq \frac{l_b}{2}$ region:

$$M(x) = \Delta F \cos \theta y_0 - \Delta F \sin \theta x + \frac{q_D l_b x}{2} - \frac{q_D x^2}{2}, \quad (27)$$

where q_D is the uniform distributed dead load per unit length and y_0 is the distance of neutral axis to the connection point of steel cable to the beam flange (half of the height of beam web).

By replacing Eq. (27) in Eq. (26), the maximum strain energy equation is obtained as follows:

$$\begin{aligned} E_{So} = & 2 \times \frac{1}{2(EI)_b} \int_0^{\frac{l_b}{2}} \left(\Delta F \cos \theta y_0 - \Delta F \sin \theta x + \frac{q_D l_b x}{2} - \frac{q_D x^2}{2} \right)^2 dx + 2 \times \frac{\Delta F^2 l_c}{2(AE)_c} \\ & + \frac{(\Delta F \cos \theta)^2 l_b}{2(AE)_b} = \frac{1}{(EI)_b} \left\{ \frac{q_D^2 l_b^5}{240} + \frac{\Delta F^2 l_b^3 \sin^2 \theta}{24} + \frac{\Delta F^2 l_b y_0^2 \cos^2 \theta}{2} \right. \\ & - \frac{\Delta F^2 l_b^2 y_0 \sin \theta \cos \theta}{4} - \frac{5 q_D \Delta F l_b^4 \sin \theta}{192} \\ & \left. + \frac{q_D \Delta F l_b^3 y_0 \cos \theta}{12} \right\} + \frac{\Delta F^2 l_c}{(AE)_c} + \frac{\Delta F^2 l_b \cos^2 \theta}{2(AE)_b}. \quad (28) \end{aligned}$$

Calculating the rate of increase in the pre-tensioning force of the cable (ΔF) through the method of least work, the relation of the whole strain energy is differentiated with respect to ΔF and the obtained result equates to zero:

$$\frac{\partial E_{So}}{\partial (\Delta F)} = 0. \quad (29)$$

The relation used for calculating the increase of pre-tensioning force of the cable (ΔF) is obtained by Eq. (30), in which μ is given in Eq. (31) (Eqs. (30) and (31) are shown in Box I). By replacing Eq. (30) in Eq. (28), the maximum strain energy of the beam E_{So} is obtained as follows:

$$\begin{aligned} E_{So} = & \frac{q_D^2}{960(EI)_b} \left\{ 4l_b^5 + 40\mu^2 l_b^3 \sin^2 \theta + 480\mu^2 l_b y_0^2 \cos^2 \theta - 240\mu^2 l_b^2 y_0 \sin \theta \cos \theta \right. \\ & - 25\mu l_b^4 \sin \theta + 80\mu l_b^3 y_0 \cos \theta + \frac{960\mu^2 (EI)_b l_c}{(AE)_c} \\ & \left. + \frac{480\mu^2 I_b l_b \cos^2 \theta}{A_b} \right\} = \frac{q_D^2 \beta}{960(EI)_b}. \quad (32) \end{aligned}$$

$$\Delta F = \frac{5q_D l_b^4 \sin \theta - 16q_D l_b^3 y_0 \cos \theta}{16 \left(l_b^3 \sin^2 \theta + 12l_b y_0^2 \cos^2 \theta - 6l_b^2 y_0 \sin \theta \cos \theta + \frac{24(EI)_b l_c}{(AE)_c} + \frac{12I_b l_b \cos^2 \theta}{A_b} \right)} = q_D \mu, \quad (30)$$

where:

$$\mu = \frac{5l_b^4 \sin \theta - 16l_b^3 y_0 \cos \theta}{16 \left(l_b^3 \sin^2 \theta + 12l_b y_0^2 \cos^2 \theta - 6l_b^2 y_0 \sin \theta \cos \theta + \frac{24(EI)_b l_c}{(AE)_c} + \frac{12I_b l_b \cos^2 \theta}{A_b} \right)}. \quad (31)$$

Box I

In Eq. (32), β is as follows:

$$\begin{aligned} \beta = & 4l_b^5 + 40\mu^2 l_b^3 \sin^2 \theta + 480\mu^2 l_b y_0^2 \cos^2 \theta \\ & - 240\mu^2 l_b^2 y_0 \sin \theta \cos \theta - 25\mu l_b^4 \sin \theta \\ & + 80\mu l_b^3 y_0 \cos \theta + \frac{960\mu^2 (EI)_b l_c}{(AE)_c} \\ & + \frac{480\mu^2 I_b l_b \cos^2 \theta}{A_b}. \end{aligned} \quad (33)$$

With regard to the symmetry of structure and loading, the maximum kinematic energy of the simply supported beam with the V-shaped pattern of cable can be determined through Eq. (4) and by replacing the maximum velocity according to Eq. (6) for half of the beam; in addition, by duplicating it, the maximum kinematic energy is determined for the whole beam as follows:

$$\begin{aligned} E_{K_o} &= 2 \times \int_0^{\frac{l_b}{2}} \frac{1}{2} m(x) (\dot{u}_o(x))^2 dx \\ &= \int_0^{\frac{l_b}{2}} m(x) (\omega_n u_o(x))^2 dx, \end{aligned} \quad (34)$$

where $m(x)$ is mass per unit length of the beam equal to $\frac{q_D}{g}$ (mass of cable is neglected) and $u_o(x)$ is the deflection curve of the simply supported beam with the V-shaped cable pattern for $0 \leq x \leq \frac{l_b}{2}$.

To determine the deflection curve, the internal bending moment should be equal to:

$$M(x) = -(EI)_b u_o''(x). \quad (35)$$

The deflection curve in Eq. (35) should satisfy the displacement boundary conditions. For the simply supported beam with the V-shaped pattern of cable, the boundary conditions for half of the beam are:

$$u_o(0) = 0, \quad u_o' \left(\frac{l_b}{2} \right) = 0.$$

By replacing Eq. (27) in Eq. (35) and imposing the above boundary conditions, the deflection curve for half of the beam is obtained as follows:

$$\begin{aligned} u_o(x) = & \frac{1}{(EI)_b} \left[\frac{q_D l_b^3 x}{24} - \frac{\Delta F l_b^2 \sin \theta x}{8} \right. \\ & + \frac{\Delta F l_b y_0 \cos \theta x}{2} - \frac{\Delta F y_0 \cos \theta x^2}{2} \\ & \left. + \frac{\Delta F \sin \theta x^3}{6} - \frac{q_D l_b x^3}{12} + \frac{q_D x^4}{24} \right]. \end{aligned} \quad (36)$$

By replacing Eq. (36) in Eq. (34), the maximum kinematic energy equation of the beam is obtained as follows:

$$\begin{aligned} E_{K_o} = & \omega_n^2 \frac{q_D}{g} \int_0^{\frac{l_b}{2}} \left(\frac{1}{(EI)_b} \left[\frac{q_D l_b^3 x}{24} - \frac{\Delta F l_b^2 \sin \theta x}{8} \right. \right. \\ & + \frac{\Delta F l_b y_0 \cos \theta x}{2} - \frac{\Delta F y_0 \cos \theta x^2}{2} \\ & \left. \left. + \frac{\Delta F \sin \theta x^3}{6} - \frac{q_D l_b x^3}{12} + \frac{q_D x^4}{24} \right] \right)^2 dx \\ = & \omega_n^2 \frac{q_D}{(EI)_b g} \left\{ \frac{31q_D^2 l_b^9}{725760} + \frac{17\Delta F^2 l_b^7 \sin^2 \theta}{40320} \right. \\ & + \frac{\Delta F^2 l_b^5 y_0^2 \cos^2 \theta}{240} - \frac{61\Delta F^2 l_b^6 y_0 \sin \theta \cos \theta}{23040} \\ & \left. - \frac{277q_D \Delta F l_b^8 \sin \theta}{1032192} + \frac{17q_D \Delta F l_b^7 y_0 \cos \theta}{20160} \right\}. \end{aligned} \quad (37)$$

By replacing Eq. (30) in Eq. (37), the maximum kinematic energy equation of the beam E_{K_o} is obtained as follows:

$$\begin{aligned} E_{K_o} = & \omega_n^2 \frac{q_D^3}{46448640 (EI)_b^2 g} \{ 1984 l_b^9 \\ & + 19584 \mu^2 l_b^7 \sin^2 \theta + 193536 \mu^2 l_b^5 y_0^2 \cos^2 \theta \\ & - 122976 \mu^2 l_b^6 y_0 \sin \theta \cos \theta - 12465 \mu l_b^8 \sin \theta \\ & + 39168 \mu l_b^7 y_0 \cos \theta \} = \omega_n^2 \frac{q_D^3 \gamma}{46448640 (EI)_b^2 g}. \end{aligned} \quad (38)$$

In Eq. (38), γ is as follows:

$$\begin{aligned} \gamma = & 1984l_b^9 + 19584\mu^2 l_b^7 \sin^2 \theta + 193536\mu^2 l_b^5 y_0^2 \cos^2 \theta \\ & - 122976\mu^2 l_b^6 y_0 \sin \theta \cos \theta - 12465\mu l_b^8 \sin \theta \\ & + 39168\mu l_b^7 y_0 \cos \theta. \end{aligned} \quad (39)$$

The natural circular frequency of the simply supported beam with the V-shaped pattern of the cable using Rayleigh's method and the principle of conservation of energy is obtained as follows:

$$\omega_n^2 = \frac{48384(EI)_b g \beta}{q_D \gamma} \rightarrow \omega_n = 48 \sqrt{\frac{21(EI)_b g \beta}{q_D \gamma}}. \quad (40)$$

Then, the natural frequency of the simply supported beam with the V-shaped pattern of the cable is determined as follows:

$$f_n = \frac{\omega_n}{2\pi} = \frac{24}{\pi} \sqrt{\frac{21(EI)_b g \beta}{q_D \gamma}}. \quad (41)$$

4.4. Calculating the natural frequency of the simply supported beam with the modified V-shaped pattern of the cable

Concerning the simply supported beam with the modified V-shaped pattern of the cable, as shown in Figure 5, the force of horizontal cable should be equal to the horizontal component of the force of the inclined cable to keep the bending moment continuous in the slope change region of the cable. Therefore, if increase in pre-tensioning force of steel cable is assumed as ΔF in the slope parts, then it will be equal to $\Delta F \cos \theta$ in the horizontal part; hence, the axial force of the beam is equal to $\Delta F \cos \theta$.

In addition, regarding symmetry of the structure and loading (as in Figure 5), the maximum strain energy of the simply supported beam with the modified V-shaped pattern of the cable for the whole beam is obtained as follows:

$$\begin{aligned} E_{So} = & 2 \times \frac{1}{2(EI)_b} \left\{ \int_0^a M_1(x)^2 dx + \int_a^{\frac{l_b}{2}} M_2(x)^2 dx \right\} \\ & + 2 \times \frac{\Delta F^2 l_c}{2(AE)_c} + \frac{(\Delta F \cos \theta)^2 (l_b - 2a)}{2(AE)_c} \\ & + \frac{(\Delta F \cos \theta)^2 l_b}{2(AE)_b}, \end{aligned} \quad (42)$$

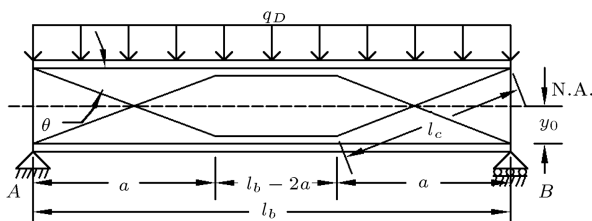


Figure 5. Simply supported beam along with the modified V-shaped cable pattern.

where a is the distance of support to the point of change in the cable slope (horizontal projection of inclined cable), and $M_1(x)$ and $M_2(x)$ are the bending moments of the simply supported beam along with the modified V-shaped pattern of the cable for $0 \leq x \leq a$ and $a \leq x \leq \frac{l_b}{2}$, respectively.

Due to symmetry of the structure and loading, the bending moment of the simply supported beam with the modified V-shaped pattern of the cable subjected to uniform distributed dead load for half of the beam is obtained as follows:

For $0 \leq x \leq a$:

$$M_1(x) = \Delta F \cos \theta y_0 - \Delta F \sin \theta x + \frac{q_D l_b x}{2} - \frac{q_D x^2}{2}. \quad (43)$$

For $a \leq x \leq \frac{l_b}{2}$:

$$M_2(x) = -\Delta F \cos \theta y_0 + \frac{q_D l_b x}{2} - \frac{q_D x^2}{2}. \quad (44)$$

By replacing Eqs. (43) and (44) in Eq. (42), the maximum strain energy is obtained as follows:

$$\begin{aligned} E_{So} = & 2 \times \frac{1}{2(EI)_b} \left\{ \int_0^a \left(\Delta F \cos \theta y_0 - \Delta F \sin \theta x + \frac{q_D l_b x}{2} - \frac{q_D x^2}{2} \right)^2 dx + \int_a^{\frac{l_b}{2}} \left(-\Delta F \cos \theta y_0 + \frac{q_D l_b x}{2} - \frac{q_D x^2}{2} \right)^2 dx \right\} \\ & + 2 \times \frac{\Delta F^2 l_c}{2(AE)_c} + \frac{(\Delta F \cos \theta)^2 (l_b - 2a)}{2(AE)_c} + \frac{(\Delta F \cos \theta)^2 l_b}{2(AE)_b} \\ = & \frac{1}{(EI)_b} \left\{ \frac{q_D^2 l_b^5}{240} + \frac{\Delta F^2 a^3 \sin^2 \theta}{3} + \frac{\Delta F^2 l_b y_0^2 \cos^2 \theta}{2} - \Delta F^2 y_0 a^2 \sin \theta \cos \theta \right. \\ & + \frac{q_D \Delta F a^4 \sin \theta}{4} - \frac{q_D \Delta F l_b a^3 \sin \theta}{3} - \frac{2q_D \Delta F y_0 a^3 \cos \theta}{3} + q_D \Delta F l_b y_0 a^2 \cos \theta \\ & \left. - \frac{q_D \Delta F l_b^3 y_0 \cos \theta}{12} \right\} + \frac{\Delta F^2 l_c}{(AE)_c} \\ & + \frac{\Delta F^2 (l_b - 2a) \cos^2 \theta}{2(AE)_c} + \frac{\Delta F^2 l_b \cos^2 \theta}{2(AE)_b}. \end{aligned} \quad (45)$$

The increase in pre-tensioning force of the cable (ΔF) calculated through the method of least work is defined

$$\Delta F = \frac{-3q_D a^4 \sin \theta + 4q_D l_b a^3 \sin \theta + 8q_D y_0 a^3 \cos \theta - 12q_D l_b y_0 a^2 \cos \theta + q_D l_b^3 y_0 \cos \theta}{4 \left(2a^3 \sin^2 \theta + 3l_b y_0^2 \cos^2 \theta - 6y_0 a^2 \sin \theta \cos \theta + \frac{3(EI)_b}{(AE)_c} [2l_c + (l_b - 2a) \cos^2 \theta] + \frac{3I_b l_b \cos^2 \theta}{A_b} \right)} = q_D \mu, \quad (46)$$

where:

$$\mu = \frac{-3a^4 \sin \theta + 4l_b a^3 \sin \theta + 8y_0 a^3 \cos \theta - 12l_b y_0 a^2 \cos \theta + l_b^3 y_0 \cos \theta}{4 \left(2a^3 \sin^2 \theta + 3l_b y_0^2 \cos^2 \theta - 6y_0 a^2 \sin \theta \cos \theta + \frac{3(EI)_b}{(AE)_c} [2l_c + (l_b - 2a) \cos^2 \theta] + \frac{3I_b l_b \cos^2 \theta}{A_b} \right)}. \quad (47)$$

Box II

by Eq. (46), in which μ is obtained by Eq. (47) (Eqs. (46) and (47) are shown in Box II). By replacing Eq. (46) in Eq. (45), the maximum strain energy of the beam E_{S_o} is obtained as follows:

$$E_{S_o} = \frac{q_D^2}{240(EI)_b} \left\{ l_b^5 + 80\mu^2 a^3 \sin^2 \theta + 120\mu^2 l_b y_0^2 \cos^2 \theta - 240\mu^2 y_0 a^2 \sin \theta \cos \theta + 60\mu a^4 \sin \theta - 80\mu l_b a^3 \sin \theta - 160\mu y_0 a^3 \cos \theta + \mu l_b y_0 a^2 \cos \theta - 20\mu l_b^3 y_0 \cos \theta + \frac{120\mu^2 (EI)_b}{(AE)_c} [2l_c + (l_b - 2a) \cos^2 \theta] + \frac{120\mu^2 I_b l_b \cos^2 \theta}{A_b} \right\} = \frac{q_D^2 \beta}{240(EI)_b}. \quad (48)$$

In Eq. (48), β is as follows:

$$\begin{aligned} \beta = & l_b^5 + 80\mu^2 a^3 \sin^2 \theta + 120\mu^2 l_b y_0^2 \cos^2 \theta \\ & - 240\mu^2 y_0 a^2 \sin \theta \cos \theta + 60\mu a^4 \sin \theta \\ & - 80\mu l_b a^3 \sin \theta - 160\mu y_0 a^3 \cos \theta \\ & + \mu l_b y_0 a^2 \cos \theta - 20\mu l_b^3 y_0 \cos \theta \\ & + \frac{120\mu^2 (EI)_b}{(AE)_c} [2l_c + (l_b - 2a) \cos^2 \theta] \\ & + \frac{120\mu^2 I_b l_b \cos^2 \theta}{A_b}. \end{aligned} \quad (49)$$

Regarding the symmetry of structure and loading, the maximum kinematic energy of the simply supported beam with the modified V-shaped cable pattern for the whole beam is obtained as follows:

$$E_{K_o} = 2 \times \left\{ \int_0^a \frac{1}{2} m(x) (\dot{u}_{o1}(x))^2 dx \right.$$

$$\left. + \int_a^{\frac{l_b}{2}} \frac{1}{2} m(x) (\dot{u}_{o2}(x))^2 dx \right\}$$

$$= \int_0^a m(x) (\omega_n u_{o1}(x))^2 dx + \int_a^{\frac{l_b}{2}} m(x) (\omega_n u_{o2}(x))^2 dx, \quad (50)$$

where $u_{o1}(x)$ and $u_{o2}(x)$ are the deflection curves of the simply supported beam with the modified V-shaped cable pattern for the $0 \leq x \leq a$ and $a \leq x \leq \frac{l_b}{2}$, respectively.

To determine the deflection curve, the internal bending moment should be equal to:

$$M_1(x) = -(EI)_b u_{o1}''(x), \quad (51)$$

$$M_2(x) = -(EI)_b u_{o2}''(x). \quad (52)$$

The deflection curve in Eqs. (51) and (52) should satisfy the displacement boundary conditions. For the simply supported beam with the modified V-shaped cable pattern, the boundary conditions for half of the beam are as follows:

$$u_{o1}(0) = 0, \quad u_{o2}'\left(\frac{l_b}{2}\right) = 0,$$

$$u_{o1}(a) = u_{o2}(a), \quad u_{o1}'(a) = u_{o2}'(a).$$

By replacing Eqs. (43) and (44) in Eqs. (51) and (52) and imposing the above boundary conditions, the deflection curve for half of the beam is obtained as follows:

For $0 \leq x \leq a$:

$$\begin{aligned} u_{o1}(x) = & \frac{1}{(EI)_b} \left[\frac{q_D l_b^3 x}{24} - \frac{\Delta F a^2 \sin \theta x}{2} \right. \\ & + 2\Delta F y_0 a \cos \theta x - \frac{\Delta F l_b y_0 \cos \theta x}{2} \\ & - \frac{\Delta F y_0 \cos \theta x^2}{2} + \frac{\Delta F \sin \theta x^3}{6} \\ & \left. - \frac{q_D l_b x^3}{12} + \frac{q_D x^4}{24} \right]. \end{aligned} \quad (53)$$

For $a \leq x \leq \frac{l_b}{2}$:

$$u_{o2}(x) = \frac{1}{(EI)_b} \left[-\frac{\Delta F a^3 \sin \theta}{3} + \Delta F y_0 a^2 \cos \theta + \frac{q_D l_b^3 x}{24} - \frac{\Delta F l_b y_0 \cos \theta x}{2} + \frac{\Delta F y_0 \cos \theta x^2}{2} - \frac{q_D l_b x^3}{12} + \frac{q_D x^4}{24} \right]. \quad (54)$$

By replacing Eqs. (53) and (54) in Eq. (50), the maximum kinematic energy of the beam is obtained as follows:

$$\begin{aligned} E_{Ko} = & \omega_n^2 \frac{q_D}{g} \left\{ \int_0^a \left(\frac{1}{(EI)_b} \left[\frac{q_D l_b^3 x}{24} - \frac{\Delta F a^2 \sin \theta x}{2} + 2\Delta F y_0 a \cos \theta x - \frac{\Delta F l_b y_0 \cos \theta x}{2} - \frac{\Delta F y_0 \cos \theta x^2}{2} + \frac{\Delta F \sin \theta x^3}{6} - \frac{q_D l_b x^3}{12} + \frac{q_D x^4}{24} \right] \right)^2 dx \right. \\ & + \int_a^{\frac{l_b}{2}} \left(\frac{1}{(EI)_b} \left[-\frac{\Delta F a^3 \sin \theta}{3} + \Delta F y_0 a^2 \cos \theta + \frac{q_D l_b^3 x}{24} - \frac{\Delta F l_b y_0 \cos \theta x}{2} + \frac{\Delta F y_0 \cos \theta x^2}{2} - \frac{q_D l_b x^3}{12} + \frac{q_D x^4}{24} \right] \right)^2 dx \Big\} \\ = & \omega_n^2 \frac{q_D}{(EI)_b^2 g} \left\{ \frac{31 q_D^2 l_b^9}{725760} - \frac{2 \Delta F^2 a^7 \sin^2 \theta}{35} + \frac{\Delta F^2 l_b a^6 \sin^2 \theta}{18} - \frac{\Delta F^2 y_0^2 a^5 \cos^2 \theta}{2} \right. \\ & + \frac{7 \Delta F^2 l_b y_0^2 a^4 \cos^2 \theta}{12} - \frac{\Delta F^2 l_b^3 y_0^2 a^2 \cos^2 \theta}{12} + \frac{\Delta F^2 l_b^5 y_0^2 \cos^2 \theta}{240} + \frac{41 \Delta F^2 y_0 a^6 \sin \theta \cos \theta}{120} \\ & - \frac{11 \Delta F^2 l_b y_0 a^5 \sin \theta \cos \theta}{30} + \frac{\Delta F^2 l_b^3 y_0 a^3 \sin \theta \cos \theta}{36} + \frac{q_D \Delta F a^8 \sin \theta}{2880} \\ & - \frac{q_D \Delta F l_b a^7 \sin \theta}{840} + \frac{q_D \Delta F l_b^3 a^5 \sin \theta}{360} \\ & \left. - \frac{q_D \Delta F l_b^5 a^3 \sin \theta}{360} - \frac{q_D \Delta F y_0 a^7 \cos \theta}{1260} \right\} \end{aligned}$$

$$+ \frac{q_D \Delta F l_b y_0 a^6 \cos \theta}{360} - \frac{q_D \Delta F l_b^3 y_0 a^4 \cos \theta}{144} + \frac{q_D \Delta F l_b^5 y_0 a^2 \cos \theta}{120} - \frac{17 q_D \Delta F l_b^7 y_0 \cos \theta}{20160} \Big\}. \quad (55)$$

By replacing Eq. (46) in Eq. (55), the maximum kinematic energy of the beam E_{Ko} is obtained as follows:

$$\begin{aligned} E_{Ko} = & \omega_n^2 \frac{q_D^3}{725760 (EI)_b^2 g} \{ 31 l_b^9 - 41472 \mu^2 a^7 \sin^2 \theta + 40320 \mu^2 l_b a^6 \sin^2 \theta - 362880 \mu^2 y_0^2 a^5 \cos^2 \theta \\ & + 423360 \mu^2 l_b y_0^2 a^4 \cos^2 \theta - 60480 \mu^2 l_b^3 y_0^2 a^2 \cos^2 \theta + 3024 \mu^2 l_b^5 y_0^2 \cos^2 \theta \\ & + 247968 \mu^2 y_0 a^6 \sin \theta \cos \theta - 266112 \mu^2 l_b y_0 a^5 \sin \theta \cos \theta \\ & + 20160 \mu^2 l_b^3 y_0 a^3 \sin \theta \cos \theta + 252 \mu a^8 \sin \theta - 864 \mu l_b a^7 \sin \theta + 2016 \mu l_b^3 a^5 \sin \theta \\ & - 2016 \mu l_b^5 a^3 \sin \theta - 576 \mu y_0 a^7 \cos \theta + 2016 \mu l_b y_0 a^6 \cos \theta - 5040 \mu l_b^3 y_0 a^4 \cos \theta \\ & + 6048 \mu l_b^5 y_0 a^2 \cos \theta - 612 \mu l_b^7 y_0 \cos \theta \} \\ = & \omega_n^2 \frac{q_D^3 \gamma}{725760 (EI)_b^2 g}. \quad (56) \end{aligned}$$

In Eq. (56), γ is as follows:

$$\begin{aligned} \gamma = & 31 l_b^9 - 41472 \mu^2 a^7 \sin^2 \theta + 40320 \mu^2 l_b a^6 \sin^2 \theta - 362880 \mu^2 y_0^2 a^5 \cos^2 \theta + 423360 \mu^2 l_b y_0^2 a^4 \cos^2 \theta \\ & - 60480 \mu^2 l_b^3 y_0^2 a^2 \cos^2 \theta + 3024 \mu^2 l_b^5 y_0^2 \cos^2 \theta + 247968 \mu^2 y_0 a^6 \sin \theta \cos \theta \\ & - 266112 \mu^2 l_b y_0 a^5 \sin \theta \cos \theta + 20160 \mu^2 l_b^3 y_0 a^3 \sin \theta \cos \theta + 252 \mu a^8 \sin \theta \\ & - 864 \mu l_b a^7 \sin \theta + 2016 \mu l_b^3 a^5 \sin \theta - 2016 \mu l_b^5 a^3 \sin \theta - 576 \mu y_0 a^7 \cos \theta \\ & + 2016 \mu l_b y_0 a^6 \cos \theta - 5040 \mu l_b^3 y_0 a^4 \cos \theta + 6048 \mu l_b^5 y_0 a^2 \cos \theta - 612 \mu l_b^7 y_0 \cos \theta. \quad (57) \end{aligned}$$

The natural circular frequency of the simply supported beam with the modified V-shaped cable pattern using Rayleigh's method and the principle of conservation of energy is obtained as follows:

$$\omega_n^2 = \frac{3024(EI)_b g \beta}{q_D \gamma} \rightarrow \omega_n = 12 \sqrt{\frac{21(EI)_b g \beta}{q_D \gamma}}. \quad (58)$$

The natural frequency of the simply supported beam with the modified V-shaped cable pattern is obtained as follows:

$$f_n = \frac{\omega_n}{2\pi} = \frac{6}{\pi} \sqrt{\frac{21(EI)_b g \beta}{q_D \gamma}}. \quad (59)$$

4.5. Calculating the natural frequency of the fixed supported beam with the V-shaped pattern of cable

In the fixed supported beam along with the V-shaped cable pattern, as shown in Figure 6, an increase in the pre-tensioning force of steel cable is equal to ΔF . Therefore, the axial force of the beam is equal to $\Delta F \cos \theta$.

Moreover, regarding the symmetry of structure and loading (as in Figure 6), the maximum strain energy of the fixed supported beam with the V-shaped cable pattern for the whole beam is determined as follows:

$$E_{So} = 2 \times \frac{1}{2(EI)_b} \int_0^{\frac{l_b}{2}} M(x)^2 dx + 2 \times \frac{\Delta F^2 l_c}{2(AE)_c} + \frac{(\Delta F \cos \theta)^2 l_b}{2(AE)_b}, \quad (60)$$

where $M(x)$ is the bending moment of the fixed supported beam with the V-shaped cable pattern for $0 \leq x \leq \frac{l_b}{2}$.

It should be mentioned that the fixed supported beam along with the V-shaped pattern of the cable has two degrees of indeterminacy (the increase in pre-tensioning force of the cable, ΔF , and the moment at fixed end, M). The increase in the pre-tensioning force of the steel cable and the fixed end moment can be calculated using the method of least work. Thus, the bending moment of the fixed supported beam with the V-shaped pattern of the cable subjected to uniform

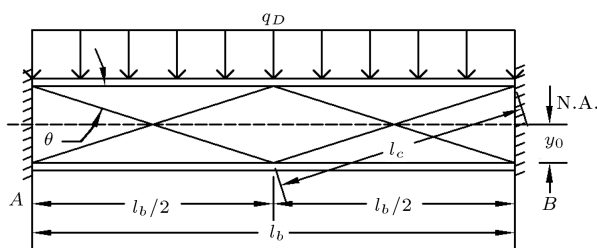


Figure 6. Fixed supported beam along with the V-shaped cable pattern.

distributed dead load for the half of beam is obtained as follows:

For $0 \leq x \leq \frac{l_b}{2}$:

$$M(x) = -M + \Delta F \cos \theta y_0 - \Delta F \sin \theta x + \frac{q_D l_b x}{2} - \frac{q_D x^2}{2}, \quad (61)$$

where M is the moment at the fixed end.

By replacing Eq. (61) in Eq. (60), the maximum strain energy formula is obtained as follows:

$$\begin{aligned} E_{So} &= 2 \times \frac{1}{2(EI)_b} \int_0^{\frac{l_b}{2}} \left(-M + \Delta F \cos \theta y_0 - \Delta F \sin \theta x + \frac{q_D l_b x}{2} - \frac{q_D x^2}{2} \right)^2 dx \\ &\quad + 2 \times \frac{\Delta F^2 l_c}{2(AE)_c} + \frac{(\Delta F \cos \theta)^2 l_b}{2(AE)_b} \\ &= \frac{1}{(EI)_b} \left\{ \frac{q_D^2 l_b^5}{240} + \frac{\Delta F^2 l_b^3 \sin^2 \theta}{24} \right. \\ &\quad + \frac{\Delta F^2 l_b y_0^2 \cos^2 \theta}{2} - \frac{\Delta F^2 l_b^2 y_0 \sin \theta \cos \theta}{4} \\ &\quad - \frac{5 q_D \Delta F l_b^4 \sin \theta}{192} + \frac{q_D \Delta F l_b^3 y_0 \cos \theta}{12} \\ &\quad + \frac{M \Delta F l_b^2 \sin \theta}{4} - M \Delta F l_b y_0 \cos \theta - \frac{q_D M l_b^3}{12} \\ &\quad \left. + \frac{M^2 l_b}{2} \right\} + \frac{\Delta F^2 l_c}{(AE)_c} + \frac{\Delta F^2 l_b \cos^2 \theta}{2(AE)_b}. \quad (62) \end{aligned}$$

Calculating the moment at the fixed end (M) through the method of least work, the relation of the whole strain energy is differentiated with respect to M and the obtained result equates to zero:

$$\frac{\partial E_{So}}{\partial M} = 0. \quad (63)$$

The calculated bending moment at the fixed end (M) is determined as follows:

$$M = \frac{q_D l_b^2}{12} - \frac{\Delta F l_b \sin \theta}{4} + \Delta F y_0 \cos \theta. \quad (64)$$

To calculate the increase of pre-tensioning force of cable (ΔF) through the method of least work, the relation of the whole strain energy is differentiated with respect to ΔF and the obtained result equates to zero:

$$\frac{\partial E_{So}}{\partial (\Delta F)} = 0. \quad (65)$$

The calculated increase of pre-tensioning force of the cable (ΔF) is obtained through Eq. (64) as follows:

$$\Delta F = \frac{q_D l_b^4 \sin \theta}{4 \left(l_b^3 \sin^2 \theta + \frac{96(EI)_b l_c}{(AE)_c} + \frac{48 I_b l_b \cos^2 \theta}{A_b} \right)} = q_D \mu. \quad (66)$$

In Eq. (66), μ is as follows:

$$\mu = \frac{l_b^4 \sin \theta}{4 \left(l_b^3 \sin^2 \theta + \frac{96(EI)_b l_c}{(AE)_c} + \frac{48 I_b l_b \cos^2 \theta}{A_b} \right)}. \quad (67)$$

If $\sin \theta = \frac{2y_0}{l_c}$ and $\cos \theta = \frac{l_b}{2l_c}$ are replaced in Eq. (64) (as in Figure 6), the fixed end moment will be the fixed end moment of the beam without cable as follows:

$$M = \frac{q_D l_b^2}{12}. \quad (68)$$

By replacing Eqs. (66) and (68) into Eq. (62), the maximum strain energy of the beam E_{So} is obtained as follows:

$$\begin{aligned} E_{So} = & \frac{q_D^2}{2880(EI)_b} \left\{ 2l_b^5 + 120\mu^2 l_b^3 \sin^2 \theta \right. \\ & + 1440\mu^2 l_b y_0^2 \cos^2 \theta - 720\mu^2 l_b^2 y_0 \sin \theta \cos \theta \\ & - 15\mu l_b^4 \sin \theta + \frac{2880\mu^2 (EI)_b l_c}{(AE)_c} \\ & \left. + \frac{1440\mu^2 I_b l_b \cos^2 \theta}{A_b} \right\} = \frac{q_D^2 \beta}{2880(EI)_b}. \end{aligned} \quad (69)$$

In Eq. (69), β is as follows:

$$\begin{aligned} \beta = & 2l_b^5 + 120\mu^2 l_b^3 \sin^2 \theta + 1440\mu^2 l_b y_0^2 \cos^2 \theta \\ & - 720\mu^2 l_b^2 y_0 \sin \theta \cos \theta - 15\mu l_b^4 \sin \theta \\ & + \frac{2880\mu^2 (EI)_b l_c}{(AE)_c} + \frac{1440\mu^2 I_b l_b \cos^2 \theta}{A_b}. \end{aligned} \quad (70)$$

Regarding the symmetry of structure and loading, the maximum kinematic energy of the fixed support beam with the V-shaped pattern of the cable for the whole beam is obtained as follows:

$$\begin{aligned} E_{Ko} = & 2 \times \int_0^{\frac{l_b}{2}} \frac{1}{2} m(x) (\dot{u}_o(x))^2 dx \\ = & \int_0^{\frac{l_b}{2}} m(x) (\omega_n u_o(x))^2 dx, \end{aligned} \quad (71)$$

where $u_o(x)$ is the deflection curve of the fixed supported beam with the V-shaped cable pattern in the range of $0 \leq x \leq \frac{l_b}{2}$.

The bending moment of the fixed supported beam with the V-shaped pattern of the cable subjected to uniformly distributed dead load in order to determine

the deflection curve for the half of beam and by replacing Eq. (68) is as follows:

$$\begin{aligned} M(x) = & -M + \Delta F \cos \theta y_0 - \Delta F \sin \theta x + \frac{q_D l_b x}{2} \\ & - \frac{q_D x^2}{2} = -\frac{q_D l_b^2}{12} + \Delta F \cos \theta y_0 \\ & - \Delta F \sin \theta x + \frac{q_D l_b x}{2} - \frac{q_D x^2}{2}. \end{aligned} \quad (72)$$

To determine the deflection curve, the internal bending moment should be equal to:

$$M(x) = -(EI)_b u_o''(x). \quad (73)$$

The deflection curve in Eq. (73) should satisfy the displacement boundary conditions. For the fixed supported beam with the V-shaped pattern of the cable, boundary conditions for the half of the beam are:

$$u_o(0) = 0, \quad u_o'(0) = u_o'\left(\frac{l_b}{2}\right) = 0.$$

By replacing Eq. (72) in Eq. (73) and imposing the above boundary conditions, the deflection curve for the half of the beam is obtained as follows:

$$\begin{aligned} u_o(x) = & \frac{1}{(EI)_b} \left[\frac{q_D l_b^2 x^2}{24} - \frac{\Delta F y_0 \cos \theta x^2}{2} \right. \\ & \left. + \frac{\Delta F \sin \theta x^3}{6} - \frac{q_D l_b x^3}{12} + \frac{q_D x^4}{24} \right]. \end{aligned} \quad (74)$$

By replacing Eq. (74) in Eq. (71), the maximum kinematic energy of the beam is obtained as follows:

$$\begin{aligned} E_{Ko} = & \omega_n^2 \frac{q_D}{g} \int_0^{\frac{l_b}{2}} \left(\frac{1}{(EI)_b} \left[\frac{q_D l_b^2 x^2}{24} - \frac{\Delta F y_0 \cos \theta x^2}{2} \right. \right. \\ & \left. \left. + \frac{\Delta F \sin \theta x^3}{6} - \frac{q_D l_b x^3}{12} + \frac{q_D x^4}{24} \right] \right)^2 dx \\ = & \omega_n^2 \frac{q_D}{(EI)_b^2 g} \left\{ \frac{q_D^2 l_b^9}{725760} + \frac{\Delta F^2 l_b^7 \sin^2 \theta}{32256} \right. \\ & + \frac{\Delta F^2 l_b^5 y_0^2 \cos^2 \theta}{640} - \frac{\Delta F^2 l_b^6 y_0 \sin \theta \cos \theta}{2304} \\ & \left. + \frac{37 q_D \Delta F l_b^8 \sin \theta}{3096576} - \frac{29 q_D \Delta F l_b^7 y_0 \cos \theta}{322560} \right\}. \end{aligned} \quad (75)$$

By replacing Eq. (66) in Eq. (75), the maximum kinematic energy formula is obtained as follows:

$$\begin{aligned} E_{Ko} = & \omega_n^2 \frac{q_D^3}{46448640(EI)_b^2 g} \{ 64l_b^9 + 1440\mu^2 l_b^7 \sin^2 \theta \\ & + 72576\mu^2 l_b^5 y_0^2 \cos^2 \theta - 20160\mu^2 l_b^6 y_0 \sin \theta \cos \theta \} \end{aligned}$$

$$\begin{aligned}
& + 555\mu l_b^8 \sin \theta - 4176\mu l_b^7 y_0 \cos \theta \} \\
& = \omega_n^2 \frac{q_D^3 \gamma}{46448640(EI)_b^2 g}. \quad (76)
\end{aligned}$$

In Eq. (76), γ is given as follows:

$$\begin{aligned}
\gamma = & 64l_b^9 + 1440\mu^2 l_b^7 \sin^2 \theta + 72576\mu^2 l_b^5 y_0^2 \cos^2 \theta \\
& - 20160\mu^2 l_b^6 y_0 \sin \theta \cos \theta + 555\mu l_b^8 \sin \theta \\
& - 4176\mu l_b^7 y_0 \cos \theta. \quad (77)
\end{aligned}$$

The natural circular frequency of the fixed supported beam with the V-shaped pattern of the cable using Rayleigh's method and the principle of conservation of energy is obtained as follows:

$$\omega_n^2 = \frac{16128(EI)_b g \beta}{q_D \gamma} \rightarrow \omega_n = 48 \sqrt{\frac{7(EI)_b g \beta}{q_D \gamma}}. \quad (78)$$

The natural frequency of the fixed supported beam with the V-shaped pattern of the cable is obtained as follows:

$$f_n = \frac{\omega_n}{2\pi} = \frac{24}{\pi} \sqrt{\frac{7(EI)_b g \beta}{q_D \gamma}}. \quad (79)$$

4.6. Calculating the natural frequency of the fixed supported beam with the modified V-shaped pattern of the cable

In the fixed supported beam with the modified V-shaped pattern of the cable, as shown in Figure 7, assuming increase in the pre-tensioning force of steel cable to be equal to ΔF in the inclined parts, increase in the pre-tensioning force of the cable in the horizontal part is $\Delta F \cos \theta$.

Therefore, the axial force of the beam is equal to $\Delta F \cos \theta$. Regarding the symmetry of structure and loading (as in Figure 7), the maximum strain energy of the fixed supported beam with the modified V-shaped pattern of the cable for the whole beam is obtained as follows:

$$\begin{aligned}
E_{So} = & 2 \times \frac{1}{2(EI)_b} \left\{ \int_0^a M_1(x)^2 dx + \int_a^{\frac{l_b}{2}} M_2(x)^2 dx \right\} \\
& + 2 \times \frac{\Delta F^2 l_c}{2(AE)_c} + \frac{(\Delta F \cos \theta)^2 (l_b - 2a)}{2(AE)_c} \\
& + \frac{(\Delta F \cos \theta)^2 l_b}{2(AE)_b}, \quad (80)
\end{aligned}$$

where $M_1(x)$ and $M_2(x)$ are the bending moments of the fixed supported beam with the modified V-shaped pattern of the cable in the $0 \leq x \leq a$ and $a \leq x \leq \frac{l_b}{2}$ ranges.

It should be mentioned that the fixed supported beam with the modified V-shaped pattern of the cable has two degrees of indeterminacy with an increase in

the pre-tensioning force of the cable (ΔF) and the moment at the fixed end (M). An increase in the pre-tensioning force of the steel cable and fixed end moment can be calculated using the method of least work. Thus, the bending moment of the fixed supported beam with the modified V-shaped pattern of the cable is obtained subjected to uniformly distributed dead load for the half of beam as follows:

For the $0 \leq x \leq a$ range:

$$\begin{aligned}
M_1(x) = & -M + \Delta F \cos \theta y_0 - \Delta F \sin \theta x \\
& + \frac{q_D l_b x}{2} - \frac{q_D x^2}{2}. \quad (81)
\end{aligned}$$

For the $a \leq x \leq \frac{l_b}{2}$ range:

$$M_2(x) = -M - \Delta F \cos \theta y_0 + \frac{q_D l_b x}{2} - \frac{q_D x^2}{2}. \quad (82)$$

By replacing Eqs. (81) and (82) in Eq. (80), the maximum strain energy is obtained as follows:

$$\begin{aligned}
E_{So} = & 2 \times \frac{1}{2(EI)_b} \left\{ \int_0^a \left(-M + \Delta F \cos \theta y_0 \right. \right. \\
& \left. \left. - \Delta F \sin \theta x + \frac{q_D l_b x}{2} - \frac{q_D x^2}{2} \right)^2 dx \right. \\
& \left. + \int_a^{\frac{l_b}{2}} \left(-M - \Delta F \cos \theta y_0 + \frac{q_D l_b x}{2} \right. \right. \\
& \left. \left. - \frac{q_D x^2}{2} \right)^2 dx \right\} + 2 \times \frac{\Delta F^2 l_c}{2(AE)_c} \\
& + \frac{(\Delta F \cos \theta)^2 (l_b - 2a)}{2(AE)_c} + \frac{(\Delta F \cos \theta)^2 l_b}{2(AE)_b} \\
= & \frac{1}{(EI)_b} \left\{ \frac{q_D^2 l_b^5}{240} + \frac{\Delta F^2 a^3 \sin^2 \theta}{3} \right. \\
& \left. + \frac{\Delta F^2 l_b y_0^2 \cos^2 \theta}{2} - \Delta F^2 y_0 a^2 \sin \theta \cos \theta \right\}
\end{aligned}$$

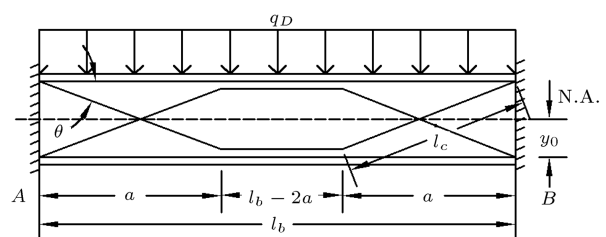


Figure 7. Fixed supported beam along with the modified V-shaped pattern of cable.

$$\begin{aligned}
& + \frac{q_D \Delta F a^4 \sin \theta}{4} - \frac{q_D \Delta F l_b a^3 \sin \theta}{3} \\
& - \frac{2q_D \Delta F y_0 a^3 \cos \theta}{3} + q_D \Delta F l_b y_0 a^2 \cos \theta \\
& - \frac{q_D \Delta F l_b^3 y_0 \cos \theta}{12} + M \Delta F a^2 \sin \theta \\
& - 4M \Delta F y_0 a \cos \theta + M \Delta F l_b y_0 \cos \theta \\
& - \frac{q_D M l_b^3}{12} + \frac{M^2 l_b}{2} \left\} + \frac{\Delta F^2 l_c}{(AE)_c} \right. \\
& + \frac{\Delta F^2 (l_b - 2a) \cos^2 \theta}{2(AE)_c} + \frac{\Delta F^2 l_b \cos^2 \theta}{2(AE)_b}. \quad (83)
\end{aligned}$$

To calculate the moment at the fixed end (M) through the method of least work, the relation of the whole strain energy is differentiated with respect to M and the obtained result equates to zero:

$$\frac{\partial E_{So}}{\partial M} = 0. \quad (84)$$

The calculated bending moment at the fixed end (M) is obtained as follows:

$$\begin{aligned}
M = & \frac{q_D l_b^2}{12} - \frac{\Delta F a^2 \sin \theta}{l_b} + \frac{4\Delta F y_0 a \cos \theta}{l_b} \\
& - \Delta F y_0 \cos \theta. \quad (85)
\end{aligned}$$

To calculate the increase in the pre-tensioning force of cable (ΔF) through the method of least work, the relation of whole strain energy is differentiated with respect to ΔF and the obtained result equates to zero:

$$\frac{\partial E_{So}}{\partial (\Delta F)} = 0. \quad (86)$$

Using Eq. (85), the calculated increase in the pre-tensioning force of the cable (ΔF) is obtained through

Eq. (87), in which μ is given by Eq. (88) (Eqs. (87) and (88) are shown in Box III).

By replacing Eqs. (85) and (87) in Eq. (83), the maximum strain energy of the beam E_{So} is obtained as follows:

$$\begin{aligned}
E_{So} = & \frac{q_D^2}{1440(EI)_b l_b} \left\{ l_b^6 - 720\mu^2 a^4 \sin^2 \theta \right. \\
& + 480\mu^2 l_b a^3 \sin^2 \theta - 11520\mu^2 y_0^2 a^2 \cos^2 \theta \\
& + 5760\mu^2 l_b y_0^2 a \cos^2 \theta + 5760\mu^2 y_0 a^3 \sin \theta \cos \theta \\
& - 2880\mu^2 l_b y_0 a^2 \sin \theta \cos \theta + 360\mu l_b a^4 \sin \theta \\
& - 480\mu l_b^2 a^3 \sin \theta + 120\mu l_b^3 a^2 \sin \theta \\
& - 960\mu l_b y_0 a^3 \cos \theta + 1440\mu l_b^2 y_0 a^2 \cos \theta \\
& - 480\mu l_b^3 y_0 a \cos \theta \\
& + \frac{720\mu^2 (EI)_b l_b}{(AE)_c} [2l_c + (l_b - 2a) \cos^2 \theta] \\
& \left. + \frac{720\mu^2 I_b l_b^2 \cos^2 \theta}{A_b} \right\} = \frac{q_D^2 \beta}{1440(EI)_b l_b}. \quad (89)
\end{aligned}$$

In Eq. (89), β is as follows:

$$\begin{aligned}
\beta = & l_b^6 - 720\mu^2 a^4 \sin^2 \theta + 480\mu^2 l_b a^3 \sin^2 \theta \\
& - 11520\mu^2 y_0^2 a^2 \cos^2 \theta + 5760\mu^2 l_b y_0^2 a \cos^2 \theta \\
& + 5760\mu^2 y_0 a^3 \sin \theta \cos \theta - 2880\mu^2 l_b y_0 a^2 \sin \theta \cos \theta \\
& + 360\mu l_b a^4 \sin \theta - 480\mu l_b^2 a^3 \sin \theta \\
& + 120\mu l_b^3 a^2 \sin \theta - 960\mu l_b y_0 a^3 \cos \theta
\end{aligned}$$

$$\Delta F = \frac{-3q_D l_b a^4 \sin \theta + 4q_D l_b^2 a^3 \sin \theta - q_D l_b^3 a^2 \sin \theta + 8q_D l_b y_0 a^3 \cos \theta - 12q_D l_b^2 y_0 a^2 \cos \theta + 4q_D l_b^3 y_0 a \cos \theta}{4 \left(\begin{aligned} & -3a^4 \sin^2 \theta + 2l_b a^3 \sin^2 \theta - 48y_0^2 a^2 \cos^2 \theta + 24l_b y_0^2 a \cos^2 \theta + 24y_0 a^3 \sin \theta \cos \theta \\ & - 12l_b y_0 a^2 \sin \theta \cos \theta + \frac{3l_b (EI)_b}{(AE)_c} [2l_c + (l_b - 2a) \cos^2 \theta] + \frac{3I_b l_b^2 \cos^2 \theta}{A_b} \end{aligned} \right)} = q_D \mu, \quad (87)$$

where:

$$\mu = \frac{-3l_b a^4 \sin \theta + 4l_b^2 a^3 \sin \theta - l_b^3 a^2 \sin \theta + 8l_b y_0 a^3 \cos \theta - 12l_b^2 y_0 a^2 \cos \theta + 4l_b^3 y_0 a \cos \theta}{4 \left(\begin{aligned} & -3a^4 \sin^2 \theta + 2l_b a^3 \sin^2 \theta - 48y_0^2 a^2 \cos^2 \theta + 24l_b y_0^2 a \cos^2 \theta + 24y_0 a^3 \sin \theta \cos \theta - 12l_b y_0 a^2 \sin \theta \cos \theta \\ & + \frac{3l_b (EI)_b}{(AE)_c} [2l_c + (l_b - 2a) \cos^2 \theta] + \frac{3I_b l_b^2 \cos^2 \theta}{A_b} \end{aligned} \right)}. \quad (88)$$

$$\begin{aligned}
& + 1440\mu l_b^2 y_0 a^2 \cos \theta - 480\mu l_b^3 y_0 a \cos \theta \\
& + \frac{720\mu^2 (EI)_b l_b}{(AE)_c} [2l_c + (l_b - 2a) \cos^2 \theta] \\
& + \frac{720\mu^2 I_b l_b^2 \cos^2 \theta}{A_b}. \quad (90)
\end{aligned}$$

Regarding symmetry of the structure and loading, the maximum kinematic energy of the fixed supported beam with the modified V-shaped pattern of the cable for the whole beam is obtained as follows:

$$\begin{aligned}
E_{Ko} &= 2 \times \left\{ \int_0^a \frac{1}{2} m(x) (\dot{u}_{o1}(x))^2 dx \right. \\
& \quad \left. + \int_a^{\frac{l_b}{2}} \frac{1}{2} m(x) (\dot{u}_{o2}(x))^2 dx \right\} \\
&= \int_0^a m(x) (\omega_n u_{o1}(x))^2 dx \\
& \quad + \int_a^{\frac{l_b}{2}} m(x) (\omega_n u_{o2}(x))^2 dx, \quad (91)
\end{aligned}$$

where $u_{o1}(x)$ and $u_{o2}(x)$ are the deflection curves of the fixed supported beam with the modified V-shaped pattern of the cable in the $0 \leq x \leq a$ and $a \leq x \leq \frac{l_b}{2}$ ranges, respectively.

By replacing Eq. (85) in Eqs. (81) and (82), the bending moment of the fixed supported beam with the modified V-shaped pattern of the cable under uniformly distributed dead load in order to determine the deflection curve for the half of beam is obtained as follows:

For the $0 \leq x \leq a$ range:

$$\begin{aligned}
M_1(x) &= -M + \Delta F \cos \theta y_0 - \Delta F \sin \theta x \\
& \quad + \frac{q_D l_b x}{2} - \frac{q_D x^2}{2} = -\frac{q_D l_b^2}{12} + \frac{\Delta F a^2 \sin \theta}{l_b} \\
& \quad - \frac{4\Delta F y_0 a \cos \theta}{l_b} + 2\Delta F \cos \theta y_0 \\
& \quad - \Delta F \sin \theta x + \frac{q_D l_b x}{2} - \frac{q_D x^2}{2}. \quad (92)
\end{aligned}$$

For the $a \leq x \leq \frac{l_b}{2}$ range:

$$\begin{aligned}
M_2(x) &= -M - \Delta F \cos \theta y_0 + \frac{q_D l_b x}{2} - \frac{q_D x^2}{2} \\
&= -\frac{q_D l_b^2}{12} + \frac{\Delta F a^2 \sin \theta}{l_b} - \frac{4\Delta F y_0 a \cos \theta}{l_b} \\
& \quad + \frac{q_D l_b x}{2} - \frac{q_D x^2}{2}. \quad (93)
\end{aligned}$$

By determining the deflection curve, the internal bending is equal to:

$$M_1(x) = -(EI)_b u_{o1}''(x), \quad (94)$$

$$M_2(x) = -(EI)_b u_{o2}''(x). \quad (95)$$

The deflection curve in Eqs. (94) and (95) should satisfy the displacement boundary conditions. For the fixed supported beam with the modified V-shaped pattern of the cable, the boundary conditions for the middle beam are:

$$u_{o1}(0) = 0, \quad u_{o1}'(0) = u_{o2}'\left(\frac{l_b}{2}\right) = 0,$$

$$u_{o1}(a) = u_{o2}(a), \quad u_{o1}'(a) = u_{o2}'(a).$$

By replacing Eqs. (92) and (93) in Eqs. (94) and (95) and imposing the above boundary conditions, the deflection curve for half of beam is obtained as follows:

For the $0 \leq x \leq a$ range:

$$\begin{aligned}
u_{o1}(x) &= \frac{1}{(EI)_b} \left[\frac{q_D l_b^2 x^2}{24} - \frac{\Delta F a^2 \sin \theta x^2}{2l_b} \right. \\
& \quad + \frac{2\Delta F y_0 a \cos \theta x^2}{l_b} - \Delta F y_0 \cos \theta x^2 \\
& \quad \left. + \frac{\Delta F \sin \theta x^3}{6} - \frac{q_D l_b x^3}{12} + \frac{q_D x^4}{24} \right]. \quad (96)
\end{aligned}$$

For the $a \leq x \leq \frac{l_b}{2}$ range:

$$\begin{aligned}
u_{o2}(x) &= \frac{1}{(EI)_b} \left[-\frac{\Delta F a^3 \sin \theta}{3} + \Delta F y_0 a^2 \cos \theta \right. \\
& \quad + \frac{\Delta F a^2 \sin \theta x}{2} - 2\Delta F y_0 a \cos \theta x \\
& \quad - \frac{\Delta F a^2 \sin \theta x^2}{2l_b} + \frac{2\Delta F y_0 a \cos \theta x^2}{l_b} \\
& \quad \left. + \frac{q_D l_b^2 x^2}{24} - \frac{q_D l_b x^3}{12} + \frac{q_D x^4}{24} \right]. \quad (97)
\end{aligned}$$

By replacing Eqs. (96) and (97) in Eq. (91), the maximum kinematic energy formula of the beam is obtained as follows:

$$\begin{aligned}
E_{Ko} &= \omega_n^2 \frac{q_D}{g} \left\{ \int_0^a \left(\frac{1}{(EI)_b} \left[\frac{q_D l_b^2 x^2}{24} - \frac{\Delta F a^2 \sin \theta x^2}{2l_b} \right. \right. \right. \\
& \quad \left. \left. + \frac{2\Delta F y_0 a \cos \theta x^2}{l_b} - \Delta F y_0 \cos \theta x^2 \right. \right.
\end{aligned}$$

$$\begin{aligned}
& + \frac{\Delta F \sin \theta x^3}{6} - \frac{q_D l_b x^3}{12} + \frac{q_D x^4}{24} \Bigg] \Bigg)^2 dx \\
& + \int_a^{l_b} \left(\frac{1}{(EI)_b} \left[-\frac{\Delta F a^3 \sin \theta}{3} \right. \right. \\
& + \Delta F y_0 a^2 \cos \theta + \frac{\Delta F a^2 \sin \theta x}{2} \\
& - 2\Delta F y_0 a \cos \theta x - \frac{\Delta F a^2 \sin \theta x^2}{2l_b} \\
& + \frac{2\Delta F y_0 a \cos \theta x^2}{l_b} + \frac{q_D l_b^2 x^2}{24} - \frac{q_D l_b x^3}{12} \\
& \left. \left. + \frac{q_D x^4}{24} \right] \right)^2 dx \Bigg\} = \omega_n^2 \frac{q_D}{(EI)_b^2 g} \left\{ \frac{q_D^2 l_b^9}{725760} \right. \\
& - \frac{\Delta F^2 a^8 \sin^2 \theta}{72l_b} - \frac{\Delta F^2 a^7 \sin^2 \theta}{42} \\
& + \frac{\Delta F^2 l_b a^6 \sin^2 \theta}{18} - \frac{\Delta F^2 l_b^2 a^5 \sin^2 \theta}{36} \\
& + \frac{\Delta F^2 l_b^3 a^4 \sin^2 \theta}{240} - \frac{2\Delta F^2 y_0^2 a^6 \cos^2 \theta}{15l_b} \\
& - \frac{2\Delta F^2 y_0^2 a^5 \cos^2 \theta}{15} + \frac{\Delta F^2 l_b y_0^2 a^4 \cos^2 \theta}{2} \\
& - \frac{\Delta F^2 l_b^2 y_0^2 a^3 \cos^2 \theta}{3} + \frac{\Delta F^2 l_b^3 y_0^2 a^2 \cos^2 \theta}{15} \\
& + \frac{4\Delta F^2 y_0 a^7 \sin \theta \cos \theta}{45l_b} \\
& + \frac{\Delta F^2 y_0 a^6 \sin \theta \cos \theta}{9} \\
& - \frac{\Delta F^2 l_b y_0 a^5 \sin \theta \cos \theta}{3} \\
& + \frac{7\Delta F^2 l_b^2 y_0 a^4 \sin \theta \cos \theta}{36} \\
& - \frac{\Delta F^2 l_b^3 y_0 a^3 \sin \theta \cos \theta}{30} + \frac{q_D \Delta F a^8 \sin \theta}{2880} \\
& - \frac{q_D \Delta F l_b a^7 \sin \theta}{840} + \frac{q_D \Delta F l_b^2 a^6 \sin \theta}{864} \\
& - \frac{q_D \Delta F l_b^3 a^5 \sin \theta}{2160} + \frac{q_D \Delta F l_b^4 a^4 \sin \theta}{6720} \\
& - \frac{q_D \Delta F y_0 a^7 \cos \theta}{1260} + \frac{q_D \Delta F l_b y_0 a^6 \cos \theta}{360}
\end{aligned}$$

$$\begin{aligned}
& - \frac{q_D \Delta F l_b^2 y_0 a^5 \cos \theta}{360} + \frac{q_D \Delta F l_b^5 y_0 a^2 \cos \theta}{720} \\
& - \frac{q_D \Delta F l_b^6 y_0 a \cos \theta}{1680} \Bigg\}. \quad (98)
\end{aligned}$$

By replacing Eq. (87) in Eq. (98), the maximum kinetic energy of the beam E_{Ko} is obtained as follows:

$$\begin{aligned}
E_{Ko} = & \omega_n^2 \frac{q_D^3}{725760(EI)_b^2 l_b g} \{ l_b^{10} - 10080\mu^2 a^8 \sin^2 \theta \\
& - 17280\mu^2 l_b a^7 \sin^2 \theta + 40320\mu^2 l_b^2 a^6 \sin^2 \theta \\
& - 20160\mu^2 l_b^3 a^5 \sin^2 \theta + 3024\mu^2 l_b^4 a^4 \sin^2 \theta \\
& - 96768\mu^2 y_0^2 a^6 \cos^2 \theta - 96768\mu^2 l_b y_0^2 a^5 \cos^2 \theta \\
& + 362880\mu^2 l_b^2 y_0^2 a^4 \cos^2 \theta \\
& - 241920\mu^2 l_b^3 y_0^2 a^3 \cos^2 \theta \\
& + 48384\mu^2 l_b^4 y_0^2 a^2 \cos^2 \theta \\
& + 64512\mu^2 y_0 a^7 \sin \theta \cos \theta \\
& + 80640\mu^2 l_b y_0 a^6 \sin \theta \cos \theta \\
& - 241920\mu^2 l_b^2 y_0 a^5 \sin \theta \cos \theta \\
& + 141120\mu^2 l_b^3 y_0 a^4 \sin \theta \cos \theta \\
& - 24192\mu^2 l_b^4 y_0 a^3 \sin \theta \cos \theta \\
& + 252\mu l_b a^8 \sin \theta - 864\mu l_b^2 a^7 \sin \theta \\
& + 840\mu l_b^3 a^6 \sin \theta - 336\mu l_b^6 a^3 \sin \theta \\
& + 108\mu l_b^7 a^2 \sin \theta - 576\mu l_b y_0 a^7 \cos \theta \\
& + 2016\mu l_b^2 y_0 a^6 \cos \theta - 2016\mu l_b^3 y_0 a^5 \cos \theta \\
& + 1008\mu l_b^6 y_0 a^2 \cos \theta - 432\mu l_b^7 y_0 a \cos \theta \} \\
= & \omega_n^2 \frac{q_D^3 \gamma}{725760(EI)_b^2 l_b g}. \quad (99)
\end{aligned}$$

In Eq. (99), γ is as follows:

$$\begin{aligned}
\gamma = & l_b^{10} - 10080\mu^2 a^8 \sin^2 \theta - 17280\mu^2 l_b a^7 \sin^2 \theta \\
& + 40320\mu^2 l_b^2 a^6 \sin^2 \theta - 20160\mu^2 l_b^3 a^5 \sin^2 \theta \\
& + 3024\mu^2 l_b^4 a^4 \sin^2 \theta - 96768\mu^2 y_0^2 a^6 \cos^2 \theta \\
& - 96768\mu^2 l_b y_0^2 a^5 \cos^2 \theta + 362880\mu^2 l_b^2 y_0^2 a^4 \cos^2 \theta
\end{aligned}$$

$$\begin{aligned}
& -241920\mu^2 l_b^3 y_0^2 a^3 \cos^2 \theta + 48384\mu^2 l_b^4 y_0^2 a^2 \cos^2 \theta \\
& + 64512\mu^2 y_0 a^7 \sin \theta \cos \theta \\
& + 80640\mu^2 l_b y_0 a^6 \sin \theta \cos \theta \\
& - 241920\mu^2 l_b^2 y_0 a^5 \sin \theta \cos \theta \\
& + 141120\mu^2 l_b^3 y_0 a^4 \sin \theta \cos \theta \\
& - 24192\mu^2 l_b^4 y_0 a^3 \sin \theta \cos \theta + 252\mu l_b a^8 \sin \theta \\
& - 864\mu l_b^2 a^7 \sin \theta + 840\mu l_b^3 a^6 \sin \theta \\
& - 336\mu l_b^6 a^3 \sin \theta + 108\mu l_b^7 a^2 \sin \theta \\
& - 576\mu l_b y_0 a^7 \cos \theta + 2016\mu l_b^2 y_0 a^6 \cos \theta \\
& - 2016\mu l_b^3 y_0 a^5 \cos \theta + 1008\mu l_b^6 y_0 a^2 \cos \theta \\
& - 432\mu l_b^7 y_0 a \cos \theta.
\end{aligned} \quad (100)$$

The natural circular frequency of the fixed supported beam with the modified V-shaped pattern of the cable using Rayleigh's method and the principle of conservation of energy is obtained as follows:

$$\omega_n^2 = \frac{504(EI)_b g \beta}{q_D \gamma} \rightarrow \omega_n = 6 \sqrt{\frac{14(EI)_b g \beta}{q_D \gamma}}. \quad (101)$$

The natural frequency of the fixed supported beam with the modified V-shaped pattern of the cable is obtained as follows:

$$f_n = \frac{\omega_n}{2\pi} = \frac{3}{\pi} \sqrt{\frac{14(EI)_b g \beta}{q_D \gamma}}. \quad (102)$$

5. Finite element modeling of steel beams prestressed with steel cable

Simply supported and fixed supported beams were designed based on Load and Resistance Factor Design (LRFD) method using AISC360-10 code [20]. Then, the natural frequency of the simply supported beam

was obtained based on the assumed shape function and also the shape function obtained from the elastic deflection curve corresponding to Eqs. (10) and (16); in addition, the natural frequency of the fixed supported beam was obtained based on the assumed shape function and the shape function derived from the elastic deflection curve corresponding to Eqs. (19) and (25), respectively. The beams were designed such that their natural frequency would be smaller than the minimum permissible frequency of 5 Hz. Table 1 shows the beam properties with different support conditions and their natural frequencies based on different assumed shape functions. It should be noted that the length of loading span was 1.5 m for the beams with different support conditions; dead and live loads were 450 and 200 kg/m² respectively.

The beams with different support conditions without cables and with different patterns of cables were modeled using ABAQUS finite element software. Figure 8 shows the finite element model of the beam with different patterns of cables. The beams and cables were modeled in 3-dimensional coordinates with shell and truss elements (as wire), respectively. The weld's connector was used to connect the cable to one of flange of the beam at two ends to constrain their corresponding degree of freedom. Moreover, the coupling constraint was applied to connect the cable to another flange of the beam so as to model the performance of the deviator. Uniformly distributed load was applied as a surface traction type on the top flange. Predefined field tool was used to create the initial pre-tensioning stress in the cable, too. In this research, mesh size was used as 5% of beam length. Figure 9 shows the position of cables in beams with different support conditions.

To better illustrate the behavior of beam with different support conditions and different patterns of the cable, first, it was modeled using the software without cable and then again, with different cable patterns; the obtained results were compared with each other.

The steel material of beams considered in this research was ST-37, yield stress 240 MPa, modulus of elasticity of steel 200 GPa, and Poisson's ratio 0.3. The material of the steel cable was found in accordance with

Table 1. Properties and natural frequency of beams with different support conditions.

Type of beam	Beam span length (m)	Cross-section of beam	Natural frequency based on assumptive shape function (Hz)	Natural frequency based on shape function of the deflection curve (Hz)	Allowable natural frequency (Hz)
Simply supported beam	4.5	IPE180	4.80	4.81	5
Fixed supported beam	10.8	IPE300	4.85	4.78	5

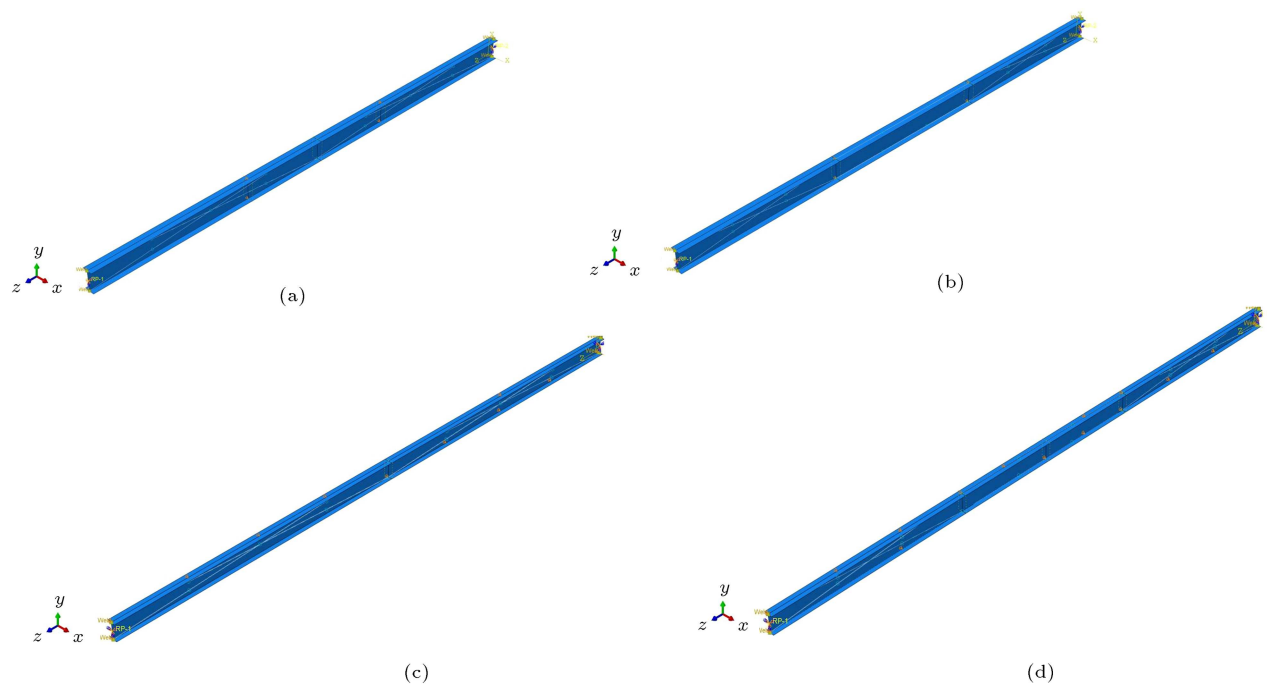


Figure 8. Finite element model of the beam along with different patterns of cable: (a) Simply supported beam along with the V-shaped pattern of cable, (b) simply supported beam along with the modified V-shaped pattern of cable, (c) fixed supported beam along with the V-shaped pattern of cable, and (d) fixed supported beam along with the modified V-shaped pattern of cable.

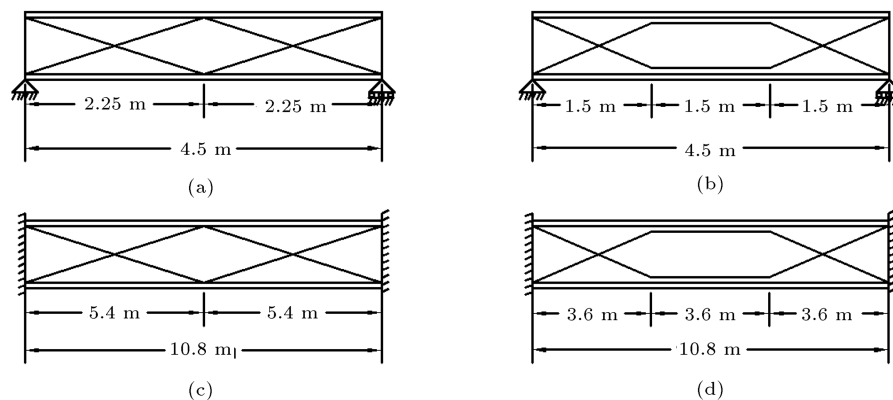


Figure 9. The locations of cables in the beams: (a) Simply supported beam along with the V-shaped pattern of cable, (b) simply supported beam along with the modified V-shaped pattern of cable, (c) fixed supported beam along with the V-shaped pattern of cable, and (d) fixed supported beam along with the modified V-shaped pattern of cable.

the ASTM A416M standard [21]. Then, 7-wire strand (grade 270 (1860)) was considered for the steel cable with low relaxation, minimum ultimate strength (f_{pu}) of 270 ksi (1860 MPa), minimum yield strength at 1% extension of 52.74 kip (234.6 KN), elasticity modulus of 28.5×10^6 psi (196501.8 MPa), and Poisson's ratio of 0.3.

6. Verification of theoretical relations of natural frequency with results of ABAQUS models

Frequency analysis of ABAQUS software was applied

so as to analyze the beams with different support conditions (Table 1) without cable and with different patterns of the cable. The 7-wire strand steel cable with low relaxation was considered for beams with different support conditions as two cables on each side of the beam web with a cross-sectional area of 140 mm^2 in accordance with ASTM A416M standards. As a result, the entire steel cable cross-section was equal to 560 mm^2 . Pre-tensioning of the steel cable was considered as 600 MPa. Controlling the accuracy of theoretical relations, the natural frequency obtained through modeling was compared to those of the theoretical relations for the beams with different support

Table 2. Natural frequency values obtained from modeling and theoretical equations for the beams with different support conditions without cable and with different cable patterns.

Type of beam		Natural frequency of beam obtained from modeling (Hz)	Natural frequency of beam obtained from theoretical equations (Hz)		Allowable natural frequency (Hz)
			Based on assumptive shape function	Based on shape function of the deflection curve	
Simply supported beam	Without cable	4.74	4.80	4.81	5
	With V-shaped cable pattern	4.83	—	4.84	
	With modified V-shaped cable pattern	5.22	—	4.98	
Fixed supported beam	Without cable	4.61	4.85	4.78	5
	With V-shaped cable pattern	4.83	—	4.86	
	With modified V-shaped cable pattern	4.92	—	4.90	

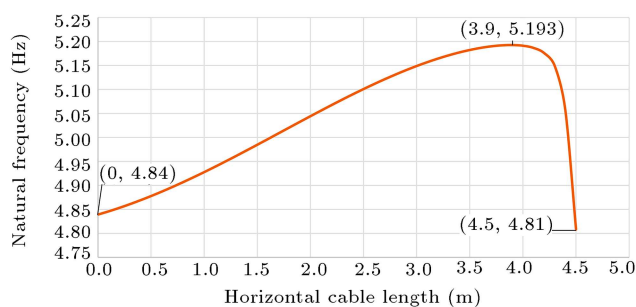
conditions and different patterns of cable. The results of the natural frequency obtained through modeling were compared with:

1. Those of Eqs. (10), (16), (41), and (59) for simply supported beams without cable and with different cable patterns;
2. With those of Eqs. (19), (25), (79), and (102) for fixed supported beams without cable and with different cable patterns, as shown in Table 2.

According to Table 2, the theoretical relations could properly predict the natural frequency of the beam. Moreover, it was observed that the natural frequency of the beam increased when the pre-tensioned steel cable rather than the beam without cable was used; therefore, using cable increases the natural frequency of the beam with different support conditions. In addition, the natural frequency of the simply supported and fixed supported beam with the modified V-shaped pattern of cable was found greater than that with the V-shaped cable pattern. As a result, the modified V-shaped cable pattern is proposed as a more appropriate pattern than the V-shaped cable pattern due to more suitable results observed.

7. The effects of horizontal cable length on natural frequency of simply supported and fixed supported beams along with the modified V-shaped cable pattern

Eqs. (59) and (102) were employed to calculate the natural frequency of simply supported and fixed supported beams along with the modified V-shaped cable pattern for 560 mm² cross-section of steel cable and at different horizontal cable lengths ($l_b - 2a$ of Figures 5 and 7). Figures 10 and 11 depict the curves of the natural

**Figure 10.** Natural frequency of simply supported beam along with the modified V-shaped pattern of cable for different horizontal cable lengths.

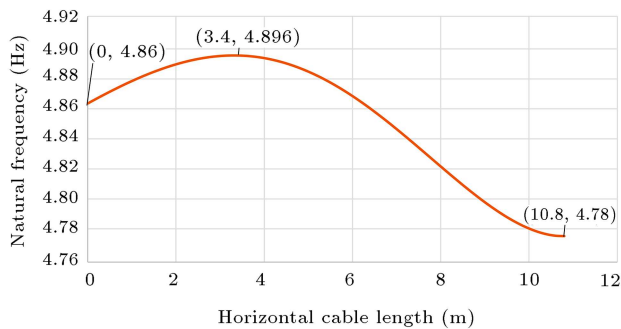


Figure 11. Natural frequency of fixed supported beam along with the modified V-shaped pattern of cable for different horizontal cable lengths.

frequency of the simply supported and fixed supported beams along with the modified V-shaped cable patterns for various lengths of the horizontal cable.

According to Figures 10 and 11, if the horizontal cable length for the simply supported and fixed supported beams along with the modified V-shaped pattern of cable is zero, their natural frequencies are 4.84 Hz and 4.86 Hz, respectively. These values are the result of natural frequency of simply supported and fixed supported beams along with the V-shaped cable pattern (Table 2). Natural frequency increases with an increase in the horizontal cable length. Finally, for horizontal cable lengths of 3.9 m and 3.4 m, the values of natural frequency are maximum at 5.193 Hz and 4.896 Hz, respectively, for the simply supported and fixed supported beams along with the modified V-shaped cable pattern. Since then, the natural frequency of the beam reduces with an increase in the horizontal cable length. The mentioned values of natural frequency are 4.81 Hz and 4.78 Hz, respectively, when the lengths of horizontal cable and beam are alike. These values are the result of natural frequency of simply supported and fixed supported beams without cable (Table 2). The reason is that for keeping the bending moment in the slope change region of the cable continuous, the force of horizontal cable should be equal to the horizontal component of the inclined cable force. Therefore, if the inclined cable becomes vertical in its special status (in the case the horizontal

cable length is equal to that of the beam length), the horizontal component of the vertical cable force equates to zero; consequently, the force of the horizontal cable becomes zero. As the length of the vertical cable, which is equal to the distance between two flanges of the beam, remains constant, no force is exerted on the length of the cable. Therefore, the cable has no effect on the beam behavior and the natural frequency of the beam is exactly similar to that of the beam without cable.

8. Sensitivity analysis on the cross-section of steel cable

To apply sensitivity analysis to the cross-section of the steel cable, different amounts of the 7-wire strand steel cable cross-section with low relaxation were considered for beams with different support conditions as an equal number of cables on both sides of the beam web with an area of 140 mm² in accordance with ASTM A416 standard and stable pre-tensioned stress of 600 MPa. Tables 3 and 4 present the natural frequency of the beams with different support conditions and different patterns of the cable modeled using ABAQUS software for different cross-sections of the steel cable.

According to Tables 3 and 4, natural frequency of the beams with different support conditions and different patterns of cable increased with an increase in steel cable cross-section area due to the increase in stiffness in the beam along with cable.

9. Sensitivity analysis on the pre-tensioning stress of the steel cable

To perform sensitivity analysis on the pre-tensioning stress of the steel cable, the 7-wire strand steel cable of beams with different support conditions with low relaxation was used in the form of four cables on each side of the beam web with an area of 140 mm² in accordance with the ASTM A16M standard. As a result, the overall steel cable cross-section is equal to 1120 mm². Table 5 presents the values of natural frequency of the beams with different support conditions and various

Table 3. Natural frequency results of simply supported beam along with different patterns of cable used in sensitivity analysis on the cross-section area of steel cable.

Total cross-section area of steel cable (mm ²)	Natural frequency of simply supported beam along with the V-shaped cable pattern (Hz)	Natural frequency of simply supported beam along with modified V-shaped cable pattern (Hz)	Allowable natural frequency (Hz)
280	4.79	5.00	5
560	4.83	5.22	5
840	4.86	5.40	5
1120	4.89	5.56	5

Table 4. Natural frequency results of fixed supported beam along with different patterns of cable used in sensitivity analysis on the cross-section area of steel cable.

Total cross-section area of steel cable (mm ²)	Natural frequency of fixed supported beam along with the V-shaped cable pattern (Hz)	Natural frequency of fixed supported beam along with modified V-shaped cable pattern (Hz)	Allowable natural frequency (Hz)
280	4.72	4.77	5
560	4.83	4.92	5
840	4.94	5.06	5
1120	5.04	5.21	5

Table 5. Natural frequency results of beams with different support conditions and different cable patterns used in sensitivity analysis on the cable pre-tensioning stress.

	Type of beam	Cable pre-tensioning stress (MPa)			Allowable natural frequency (Hz)
		400	600	800	
Simply supported beam	Along with the V-shaped pattern	4.89	4.89	4.89	5
	Along with the modified V-shaped cable pattern	5.56	5.56	5.56	
Fixed supported beam	Along with the V-shaped cable pattern	5.04	5.04	5.04	5
	Along with the modified V-shaped cable pattern	5.21	5.21	5.21	

patterns of the cable modeled using ABAQUS software for different values of pre-tensioning of the steel cable.

According to Table 5, the natural frequency of beams with different support conditions and different patterns of cable remained stable with an increase in the pre-tensioning stress of steel cable.

10. Conclusion

Due to their low weights, small cross-sections, and high tensile strengths, cables can be proper alternatives for pre-tensioning the steel beams subjected to external loads. In this research, cables were employed to prestress the beams with different support conditions in which the natural frequency was not within the allowable range despite their appropriate design under bending and shear. Theoretical equations were used to calculate the rate of increase in pre-tensioning force of the cable as well as the natural frequency of the simply supported and fixed supported beams with and without cable. The results obtained from the finite element model and theoretical equations are briefly summarized as follows:

1. The moment at the end of the fixed supported beam with the V-shaped pattern of cable was equal

to that at the end of the beam without cable ($\frac{qL^2}{12}$); however, in the fixed supported beam along with the modified V-shaped pattern of cable, the moment at fixed end was dependent on external loading and total force of the cable, too;

2. Comparison between the results of theoretical equations and those of finite element model demonstrated that the theoretical equations developed in this article could properly predict the natural frequency of the simply supported and fixed supported beams without cable and along with different patterns of cable;
3. Adding cable to the beam resulted in increasing the natural frequency of the beam with different support conditions and different patterns of cable;
4. The natural frequency of the simply supported and fixed supported beams along with the modified V-shaped cable pattern was higher than that with the V-shaped pattern. Therefore, the modified V-shaped pattern of cable can be a more appropriate pattern;
5. The effects of horizontal cable length on the natural frequency of simply supported and fixed supported beams along with the modified V-shaped pattern of cable were studied. According to the obtained

results, if the length of horizontal cable remains equal to zero, the natural frequency of beam along with the V-shaped pattern of cable was obtained. If the length of horizontal cable increased, natural frequency increased. With an increase in the length of horizontal cable, natural frequency decreased, too. When the lengths of the horizontal cable and beam were equal, the natural frequency results of the simply supported and fixed supported beams without cable were obtained;

6. In beams with different support conditions and different patterns of cable, the natural frequency increased upon increasing the cross-section of steel cable, considering equal pre-tensioning. Moreover, proper values of steel cable cross-sections were obtained, as per which the natural frequency criterion of beams with different support conditions and different patterns of cable was satisfied;
7. By increasing the pre-tensioning in the steel cables of equal cross-sections, the natural frequency of the beams with different support conditions and different patterns of cable was found constant.

Nomenclature

$u(x, t)$	Simple harmonic motion of a beam under free vibration
$\psi(x)$	Shape function
z_o	Amplitude of generalized coordinate
$z(t)$	
ω_n	Natural circular frequency
E_{S_o}	Maximum strain energy
$u_o(x)$	Maximum displacement
E_{K_o}	Maximum kinematic energy
$m(x)$	Mass per unit length of the beam
$EI(x)$	Flexural rigidity
L	Beam length
q_D	Uniform distributed dead load per unit length
g	Gravity acceleration
f_n	Natural frequency
$M(x)$	Bending moment
F_{pt}	Pre-tensioning force of the steel cable
ΔF	Increase in pre-tensioning force of the steel cable
Δl	Increase in length of steel cable
l_b	Beam length
l_c	Inclined cable length
A_b	Cross-section area of beam
A_c	Cross-section area of cable on both sides of the web

E_b	Elasticity modulus of beam
E_c	Elasticity modulus of cable
I_b	Moment of inertia of beam
θ	Angle of inclined cable with the horizontal axis
y_0	Distance of neutral axis to the connection point of steel cable to the beam flange (half of the height of beam web)

References

1. Razavi, M. and Sheidaii, M.R. "Seismic performance of cable zipper-braced frames", *Journal of Constructional Steel Research*, **74**, pp. 49–57 (2012).
2. Hou, X. and Tagawa, H. "Displacement-restraint bracing for seismic retrofit of steel moment frames", *Journal of Constructional Steel Research*, **65**, pp. 1096–1104 (2009).
3. Fanaie, N., Aghajani, S., and Afsar Dizaj, E. "Theoretical assessment of the behavior of cable bracing system with central steel cylinder", *Advances in Structural Engineering*, **19**(3), pp. 463–472 (2016).
4. Fanaie, N., Aghajani, S., and Afsar Dizaj, E. "Strengthening of moment-resisting frame using cable-cylinder bracing", *Advances in Structural Engineering*, **19**(11), pp. 1–19 (2016).
5. Giaccu, G.F. "An equivalent frequency approach for determining non-linear effects on pre-tensioned-cable cross-braced structures", *Journal of Sound and Vibration*, **422**, pp. 62–78 (2018).
6. Troitsky, M.S., *Prestressed Steel Bridges-Theory and Design*, Van Nostrand Reinhold, New York (1990).
7. Le, T.D., Pham, T.M., Hao, H., et al. "Flexural behaviour of precast segmental concrete beams internally prestressed with unbonded CFRP tendons under four-point loading", *Engineering Structures*, **168**, pp. 371–383 (2018).
8. Pisani, M.A. "Behaviour under long-term loading of externally prestressed concrete beams", *Engineering Structures*, **160**, pp. 24–33 (2018).
9. Lou, T., Lopes, S.M.R., and Lopes, A.V. "Effect of linear transformation on nonlinear behavior of continuous prestressed beams with external FRP cables", *Engineering Structures*, **147**, pp. 410–424 (2017).
10. Nie, J.G., Cai, C.S., Zhou, T.R., et al. "Experimental and analytical study of prestressed steel-concrete composite beams considering slip effect", *Journal of Structural Engineering*, **133**(4), pp. 530–540 (2007).
11. Zhou, H., Li, S., Chen, L., et al. "Fire tests on composite steel-concrete beams prestressed with external tendons", *Journal of Constructional Steel Research*, **143**, pp. 62–71 (2018).
12. Belletti, B. and Gasperi, A. "Behavior of prestressed steel beams", *Journal of Structural Engineering*, **136**(9), pp. 1131–1139 (2010).

13. Park, S., Kim, T., Kim, K., et al. “Flexural behavior of steel I-beam prestressed with externally unbonded tendons”, *Journal of Constructional Steel Research*, **66**, pp. 125–132 (2010).
14. Kambal, M.E.M. and Jia, Y. “Theoretical and experimental study on flexural behavior of prestressed steel plate girders”, *Journal of Constructional Steel Research*, **142**, pp. 5–16 (2018).
15. Zhang, W.F. “Symmetric and antisymmetric lateral-torsional buckling of prestressed steel I-beams”, *Thin-Walled Structures*, **122**, pp. 463–479 (2018).
16. Noble, D., Nogal, M., O'Connor, A., et al. “Dynamic impact testing on post-tensioned steel rectangular hollow sections; An investigation into the “compression-softening” effect”, *Journal of Sound and Vibration*, **355**, pp. 246–263 (2015).
17. Cao, L., Liu, J., and Chen, Y.F. “Vibration performance of arch prestressed concrete truss girder under impulse excitation”, *Engineering Structures*, **165**, pp. 386–395 (2018).
18. Miyamoto, A., Tei, K., Nakamura, H., et al. “Behavior of prestressed beam strengthened with external tendons”, *Journal of Structural Engineering*, **126**(9), pp. 1033–1044 (2000).
19. Park, Y.H., Park, C., and Park, Y.G. “The behavior of an in-service plate girder bridge strengthened with external prestressing tendons”, *Engineering Structures*, **27**, pp. 379–386 (2005).
20. American Institute of Steel Construction (AISC) ANSI/AISC360—10, *Specification for Structural Steel Buildings*, Chicago, IL (2010).

21. American Society for Testing and Materials (ASTM), *Standard Specification for Low-Relaxation, Seven-Wire Steel Strand for Prestressed Concrete* (ASTM A416M), Philadelphia, Pa (2018).

Biographies

Nader Fanaie obtained his BS, MS, and PhD degrees in Civil Engineering from the Department of Civil Engineering at Sharif University of Technology, Tehran, Iran. He graduated in 2008 and, at present, is a faculty member at K. N. Toosi University of Technology, Tehran, Iran. He has supervised 38 MS theses up to now. His field of research includes seismic hazard analysis, earthquake simulation, seismic design, and IDA. He has published about 70 journal and conference papers and also 13 books. He ranked the 3rd in the first mathematical competition held at Sharif University of Technology in 1996 and received a Gold Medal in “The 4th Iranian Civil Engineering Scientific Olympiad” in 1999. In 2001, he achieved the first rank in the exam of PhD scholarship abroad. He has also been acknowledged as an innovative engineer on ‘Engineering Day’ in 2008.

Fatemeh Partovi received her BS and MS degrees in Civil engineering from the Department of Civil Engineering at K. N. Toosi University of Technology, Tehran, Iran. She graduated in 2017. She achieved 4th and 2nd ranks in her undergraduate and graduate classes, respectively. She has published multiple papers in Journals of Central South University, Scientia Iranica, and Constructional Steel Research.